Metabolic Engineering of *Lactococcus lactis* to Enhance Biopolymer Bead Production

A thesis presented in partial fulfilment of the
requirements of the degree of
Master of Science
in
Microbiology
at Massey University, Palmerston North,
New Zealand.

Lydia Shivonne-Lee Hume
2012

Abstract

Polyhydroxyalkanoates (PHAs) are a group of biopolyesters that are synthesized by polyester synthases in a wide range of Gram-positive and Gram-negative bacteria, and are stored in bacterial cells as intracellular inclusions. Recently, these inclusions have been considered for biotechnological and biomedical applications as surface-functionalized micro-/nanobeads. The production of functionalized poly[(*R*)-3-hydroxybutyrate] (PHB; a biopolyester) beads in the food-grade host *Lactococcus lactis* has recently been established, however the levels of PHB production are low in comparison to levels produced by recombinant *E. coli*. In an attempt to improve PHB production in *L. lactis*, the metabolic flux of carbon from pyruvate was engineered to redirect the flux towards acetyl Co-A, one of the precursors for PHB. This involved knocking out two enzymes involved in conversion of acetyl Co-A to acetate and ethanol (acetaldehyde dehydrogenase and phosphate acetyltransferase, respectively). PHB production using a strain deficient in acetaldehyde dehydrogenase (*adhE*) was not assessed due to difficulties encountered in creating the knockout strain. This study showed the successful construction and phenotypic characterisation of a phosphate acetyltransferase (*eutD*) deficient strain of *L. lactis*. Production of acetate was substantially reduced in this mutant, and growth of the strain was improved when PHB production was established. However, rather than increasing, levels of PHB production by the *eutD* knockout were comparable to WT. Additionally, complementation of the mutant strain still needs to be achieved to confirm that the observed acetate-production phenotype is attributable to the lack of the *eutD* gene.

Acknowledgements

First of all, I would like to thank my supervisor Bernd Rehm for the the opportunity to do my Masters qualification under his supervision. I would also like to give a special thanks to Bernd, Jason Lee, Jenny Draper and Anika Jahns for their time, guidance and encouragement throughout my degree.

Thanks to Katrin Grage and Jenny for feedback on my thesis. Thanks to everybody in Rehmlab and IMBS who offered me their time, support and technical expertise when needed.

Thanks to my friends and family for keeping me sane, thanks to Alby for being awesome over the past few years, and a special thanks to my parents Owen and Carey Hume for their unwavering support and encouragement.

“A little more persistence, a little more effort, and what seemed hopeless failure may turn to glorious success”

Abbreviations

°C	Degree Celsius
3HB	3-hydroxybutyrate
AGE	Agarose Gel Electrophoresis
BSA	Bovine serum albumin
DMSO	Dimethyl sulfoxide
GC/MS	Gas chromatography mass spectrometry
LDH	Lactate dehydrogenase
PHA	Polyhydroxyalkanoate
PhaC	PHA synthase
PHB	Polyhydroxybutyrate
RE	Restriction endonuclease
WT	Wildtype

List of Figures

List of tables

Chapter 1: Introduction

1.1 Polyhydroxyalkanoates (PHAs)

Polyhydroxyalkanotates (PHAs) are a group of biopolyesters that are produced naturally by many bacteria under nutrient-limiting conditions when carbon is in excess. PHAs are synthesized by polyester synthase enzymes and stored as insoluble spherical inclusions in the cytoplasm of the bacteria. These inclusions act as a biodegradable carbon source for the cell during later periods of starvation. Recently, there has been considerable interest in the application of PHAs in biomedical and biotechnological fields due to their valuable properties such as biodegradability, biocompatibility, and generation from renewable resources, and modifiable thermal and physical characteristics. One of the most common biopolyesters, poly[(*R*)-3-hydroxybutyrate] (PHB), has recently been considered for use as functionalized beads, exploiting the natural spherical structure of PHB inclusions. Some of the potential applications for functionalized PHB beads include bioseparation, protein purification, targeted drug delivery, molecular imaging, diagnostics, and enzyme immobilization (Grage et al., 2009).

1.1.1 Biosynthesis and Formation of PHB Granules

PHA inclusions consist of a biopolyester core surrounded by a phospholipid monolayer shell with embedded and attached proteins, including the polyester synthases. Biogenesis of PHB is carried out by the three enzymes *β*-ketothiolase, acetoacetyl-CoA reductase, and PHA synthase (PhaA, PhaB, and PhaC respectively; Figure 3). *β*-ketothiolase catalyzes the condensation of two molecules of acetyl CoA to generate acetoacetyl CoA, which is reduced to *(R)*-3-hydroxybutyryl CoA by the NADPH-dependent acetoacetyl-CoA reductase (Rehm, 2006). The polyester synthase then polymerizes the *(R)*-hydroxyacyl-CoA thioesters into polyesters with the simultaneous release of CoA. The polyester synthase remains attached to the polyester granules it generates, and can be engineered to perform a range of functions, such as a display of binding domains

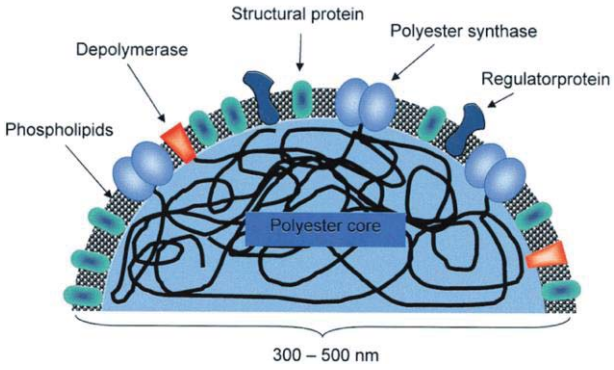

Figure 1. Schematic representation of a biopolyester granule with associated proteins (Rehm, 2003).

applicable for affinity purification (Mifune et al., 2009). In many bacteria, the three genes involved in PHB biosynthesis are located in a single operon, *pha*CAB; recombinant expression of these genes in a range of host organisms results in biopolyester production (Jo et al., 2006; Lee et al., 1994; Mifune et al., 2009).

Currently there are two models for how the granules self-assemble inside bacteria; the micelle model and the budding model (Figure 2). The micelle model is supported by *in vitro* granule assembly where the polyester synthase is assumed to be soluble, becoming amphipathic as it polymerizes the polyester chain. The polyester chain becomes increasingly hydrophobic as it lengthens, eventually aggregating with other synthase-polyester molecules to form a granule with the hydrophobic polyester chains at the core and the polyester synthases convalently attached at the surface (Rehm, 2006). The budding model proposes that the polyester synthase is associated with the cytoplasmic membrane, synthesizing the polyester chains into the intermembrane space. The extending chains would accumulate in the membrane, eventually budding off to form an inclusion body surrounded by a phospholipid monolayer.

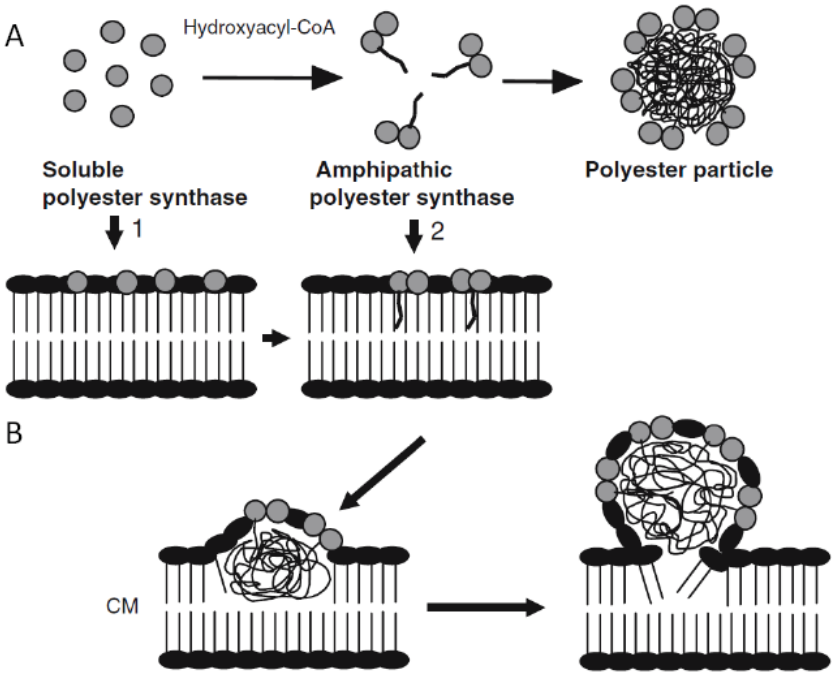

Figure 2. Models for PHA bead self-assembly. (A) Micelle model and (B) Budding model for PHA granule self-assembly. 1 and 2 indicate potential routes for *in vivo* granule assembly (Rehm, 2006).

1.1.2 Applications of PHB Granules

The various properties of PHAs including biodegradability, biocompatibility, and generation from renewable resources makes them a potential candidate for many biomedical and biotechnological applications. One of the drawbacks of PHAs is that they are naturally rather brittle, limiting their use. However, processes such as chemical modification or generation of copolymers can improve the material properties. The selection of an appropriate production strain, as well as adjusting the growth conditions and carbon levels, allows PHAs with desirable compositions to be generated. For example, PHAs that are less brittle, more flexible, and have increased hydrophilicity whilst maintaining their tensile strength are important for certain medical applications (Hazer and Steinbuchel, 2007). PHB granules have the advantage of the general properties of PHA, as well as being naturally spherical in shape. This spherical structure has recently been exploited by researchers. The nano-scale size and shell-core composition of PHB granules allow a wide range of applications for the beads in biotechnology and biomedicine (Chen and Wu, 2005; Grage et al., 2009).

One of the applications of PHB granules is affinity purification of biological molecules. For example, beads that display an antibody at their surface at high density have higher binding affinity than the antibody itself, demonstrating potential for enhancing the sensitivity of diagnostic assays (Soukka et al., 2001). A second application is the use of nano-beads in biomedicine, for example in targeted drug delivery, target specific therapy, molecular imaging and biomarkers/biosensors for diagnostics (Grage et al., 2009). In targeted drug delivery and target-specific therapy nano-beads are capable of delivering a vast range of therapeutic agents, demonstrating enormous potential as an efficient and safe drug delivery system (Panyam and Labhasetwar, 2003). Functionalized beads displaying viral or bacterial antigens can also be used as a vaccine delivery system (Parlane et al., 2011; Parlane et al., 2012). Nano-beads have also been used as contrast agents for imaging applications and optical switches for triggered release of drugs and therapy (Jiang et al., 2004). An example of the use of nanoparticles in diagnosis is the detection and identification of single DNA or protein molecules by labelling the molecules with nanoparticles, and detecting blockages in ionic current when passed through a nanopipette (Karhanek et al., 2005). These various examples

demonstrate the significant potential for surface-functionalized PHB beads in a range of applications and encourage further research surrounding PHB production and development.

1.2 Production in Gram-positive hosts

The production of functionalized polyester beads has been explored by a number of groups (Backstrom et al., 2007; Banki et al., 2005; Barnard et al., 2005; Zou and Chen, 2007), but until recently they had only been produced in Gram-negative bacteria. The issue with using Gram-negative bacteria to produce beads for biomedical applications is that they contain lipopolysaccharides (LPS) which act as endotoxins in humans. These toxins are co-purified with the beads when produced in gram-negative hosts; numerous purification steps need to be carried out to remove the endotoxins to U.S. Food and Drug Administration (FDA) approved levels (Mifune et al., 2009). There are methods in place for the depyrogenation of the plastic PHA; however these methods are considered too harsh for the surface functionalities of PHB beads (Mifune et al., 2009). Therefore, to produce beads for medical applications, it would be beneficial to use a production strain that does not produce LPS or any other byproduct that is harmful to humans. It was this issue that led to the investigation of PHB bead production in gram-positive organisms, as they lack the harmful LPS.

There are a number of Gram-positive bacteria that have been shown to naturally accumulate PHAs; among them are *Bacillus* spp., *Clostridium* spp., *Corynebacterium* spp., *Nocardia* spp., *Rhodococcus* spp., *Streptomyces* spp. and *Staphylococcus* spp. (Valappil et al., 2007). However, these natural PHA producers often have long generation times, can frequently be hard to lyse, and contain PHA degradation pathways. Therefore it is beneficial to establish PHA pathways in Gram-positive organisms that do not naturally make PHA, thus generating production strains which utilize multiple substrates, lack PHA degradation pathways, and have shorter generation times. One of the first reported productions of endotoxin-free PHB in a recombinant Gram-positive host was achieved by expression of the *pha*CAB operon derived from *Ralstonia eutropha* in *Corynebacterium glutamicum* (Jo et al., 2006). More recently, *Lactococcus lactis* was engineered to recombinantly produce endotoxin-free

functionalized PHB beads that displayed surface-immobilized IgG binding domains (Mifune et al., 2009).

1.3 *Lactococcus lactis*

L. lactis is a non-pathogenic bacterium belonging to a group of microorganisms called lactic acid bacteria (LAB), which are commonly used in the production of fermented dairy products such as yoghurt and cheese. *L. lactis* is a food-grade, generally-regarded-as-safe (GRAS) organism and thus is suitable for use in biomedical applications. There are also many genetic tools available for *L. lactis* including transformation, gene integration, gene knockout, the availability of numerous vectors, and constitutive and regulated gene expression systems (Mierau and Kleerebezem, 2005). Arguably the most valuable of these genetic tools is the nisin-controlled gene expression system (NICE); this system allows for the inducible expression of a gene of interest when placed under the control of the inducible promoter P_{nisA} on a plasmid or on the chromosome, by the addition of nisin (Mierau and Kleerebezem, 2005). *L. lactis* is not a natural producer of PHB; however, as previously mentioned, a PHB biogenesis pathway has been successfully established in this organism that allows for the production of surface-functionalized PHB beads (Mifune et al., 2009). The plasmid pNZ-CAB, containing the codon-optimized PHB operon *pha*CAB under P_{nisA} control, and the empty control plasmid pNZ-8148 were used to establish PHB production in *L. lactis* (Mifune et al., 2009). However, although it has been shown that recombinant *L. lactis* can produce PHB, the yields reported were considerably less (6% wt/wt of its cellular dry weight (CDW)) than those achieved for recombinant *E. coli* and *C. necator* (60-80% wt/wt) and recombinant *C. glutamicum* (50% wt/wt) (Jo et al., 2007; Madison and Huisman, 1999; Mifune et al., 2009). This suggests that the metabolism of *L. lactis* does not favour PHB production and further research into the engineering of *L. lactis* metabolic fluxes may be able to increase PHB accumulation.

1.3.1 *Lactococcus Metabolism and Metabolic Engineering*

Use of *L. lactis* for recombinant protein production has the benefit of a relatively small sequenced genome (~2.5 Mb), a simple metabolism and industrial relevance. In particular, *L. lactis* is used in the food industry for the production of enzymes, protein or

peptide ingredients and therapeutic proteins (De Vos and Hugenholtz, 2004). However many of these desired metabolites are not efficiently produced and are therefore a prime target for metabolic engineering aimed at optimizing or increasing their yield.

Metabolic engineering provides insight into the functioning of the many different cellular pathways that exist in living cells. There have been many studies carried out that look at predictive modelling of cellular pathways using completed genomes and the effects of gene knockouts on metabolic fluxes (Hoefnagel et al., 2002a; Papin et al., 2003; Sanford et al., 2002). The next step is to validate these predictions experimentally, then optimize and apply them to the appropriate systems.

In order to best achieve this, it is important to understand the metabolic fluxes involved in producing the desired product. Metabolic energy in *L. lactis* is generated through the final stage of glycolysis, in which substrate level phosphorylation occurs, and pyruvate is reduced to lactate by a lactate dehydrogenase (LDH) (De Vos and Hugenholtz, 2004). Redirecting this carbon flux toward the accumulation of desired products, whilst maintaining the overall physiology of the cell, is a complex task. This glycolytic pathway, including the sequential pyruvate pathway, has been studied by a number of groups (Cocaign-Bousquet et al., 2002; Hoefnagel et al., 2002b; Starrenburg and Hugenholtz, 1991) and a metabolic model has been established.

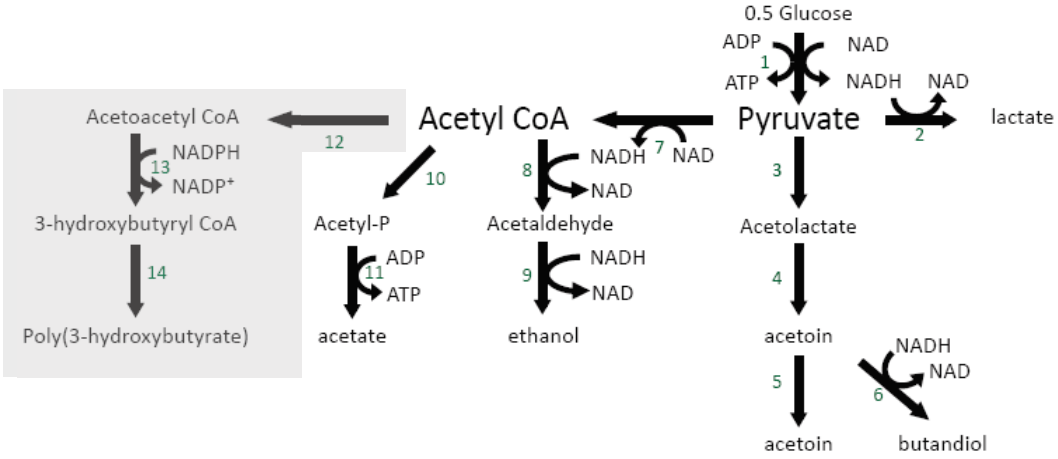

Figure 3. Distribution of carbon from pyruvate in *L. lactis* under aerobic conditions. The shaded area includes steps that take place when PHB synthesis is induced. Numbers indicate the following enzymes or steps: 1, glycolysis; 2, lactate dehydrogenase; 3, acetolactate synthase; 4, acetolactate decarboxylase; 5, acetoin efflux; 6, acetoin dehydrogenase; 7, pyruvate dehydrogenase; **8, acetaldehyde dehydrogenase**; 9, alcohol dehydrogenase; **10, phosphate acetyltransferase**; 11, acetate kinase; 12, β-ketothiolase (PhaA); 13, acetoacetyl CoA reductase (PhaB); 14, PHB synthase (PhaC). Enzymes targeted in this study are indicated in bold above. Modified from (Hoefnagel et al., 2002a).

A number of enzymes involved in the pyruvate pathway have been studied for assignment of functionality and also to study the effects of over-expression or knockouts on the carbon flux. It is important to note that metabolism is a highly complex system that is connected not just through carbon metabolites but also through electron carriers [NAD(P)H] and Gibbs free energy (ATP) carriers (Hoefnagel et al., 2002a). In an *ldh*$^-$ strain of *L. lactis* (NZ9010), the carbon flux was redirected such that during fermentation under aerobic conditions lactate production was almost non-existent (1.5% of total pyruvate converted compared with 72.1% in wild type NZ9000) and acetoin was the main end product (60.7% compared with undetectable amounts in NZ9000); additionally, the production of acetate and ethanol under these same conditions increased from 14.7% to 22.8% (Bongers et al., 2003). Over-expression of the α-acetolactate synthase also increased production of acetoin; however lactate was still the main end product of fermentation (Platteeuw et al., 1995). Interestingly, over-expression of this same α-acetolactate synthase enzyme in and *ldh*$^-$ strain of *L. lactis* did not significantly alter levels of acetoin, suggesting that *ldh*$^-$ strains already accumulate the maximal level of acetoin tolerated by the cells (Platteeuw et al., 1995). In an acetaldehyde/alcohol dehydrogenase deficient (*adhE*-) strain of *L. lactis*, the carbon flux from pyruvate was rerouted such that only small amounts of acetaldehyde and no ethanol was produced (Arnau et al., 1998). However this study did not measure the

levels of any other fermentation products, which limits its contribution to analysis of the pyruvate pathway and effects of knockouts.

These studies provide valuable insight into the pyruvate pathway, and further analysis of this pathway, among others, will increase the reliability and accuracy of predictive models and enable effective engineering strategies to be designed. For example, one of the precursors for PHB is acetyl CoA; however there has not been any significant research into engineering the pyruvate carbon flux for acetyl CoA accumulation. The majority of *L. lactis* metabolic engineering has focused on redirecting pyruvate metabolism towards products with considerable economic value such as food flavourings, for example diacetyl (De Vos and Hugenholtz, 2004; Swindell et al., 1996). Further research into engineering of the pyruvate metabolism to increase accumulation of acetyl CoA could potentially improve PHB production in *L. lactis*. A previous study revealed that when the lactate dehydrogenase encoding gene is knocked out, lactate levels in the culture media significantly decrease and the acetate levels significantly increase (Lee, 2011). Examination of the enzymes involved in the distribution of carbon from pyruvate, specifically enzymes involved in pathways from acetyl CoA, revealed two candidate enzymes that if knocked out, may increase the accumulation of acetyl CoA and consequently PHB. The enzymes chosen were the phosphate acetyltransferase enzyme (encoded by *eutD*) involved in the acetate pathway and the acetaldehyde dehydrogenase enzyme (encoded by *adhE*) involved in the acetaldehyde pathway (enzymes in bold in Figure 3). This study looks at the effects of knocking out the *adhE* and *eutD* genes on *L. lactis* in relation to PHB accumulation and fermentation products.

1.4 Aim of this study

The purpose of this study is to create mutant strains of *L. lactis* NZ9000 in which either the phosphate acetyltransferase encoding gene (*eutD*) or the acetaldehyde dehydrogenase encoding gene (*adhE*) are knocked out.

The target genes will be interrupted by replacing an internal gene segment with an antibiotic resistance gene. Knockouts will be confirmed by PCR analysis and restriction enzyme digest.

This project also aims to establish PHB production in the mutant strains of *L. lactis* NZ9000, using the plasmids pNZ-CAB and pNZ-8148. PHB production will be assessed by GC/MS analysis. In addition to PHB, the acetate and lactate levels of the strains will also be assessed in order to characterise the strains and gene function.

CHAPTER 2: MATERIALS AND METHODS

Unless specified, all reagents were purchased from Sigma-Aldrich, Ajax Finechem or Merck.

2.1 Strains and Plasmids

The tables below list the strains and plasmids used in this study.

2.1.1 Strains

Table 1. Bacterial strains used in this study

Strain	Relevant characteristics	Source
Escherichia coli		
TOP10	F⁻ *mcr*A Δ(*mrr-hsd*RMS-*mcr*BC) ϕ80*lacZ*ΔM15 Δ*lac*X74 *rec*A1 *ara*D139 Δ(*ara-leu)*7697 *gal*U *gal*K *rps*L (Str^r) *end*A1 *nup*G	Invitrogen
XL1-Blue	*recA1 endA1 gyrA96 thi-1 hsdR17 supE44 RelA1 lac* [F' *proAB lacI^{q}ZΔM15* Tn*10* (Tet^r)]	Novagen
Lactococcus lactis		
NZ9000	MG1363 derivative, *pepN*::*nisRK*	(Hoefnagel et al., 2002a)
NZ9010	NZ9000 derivative, *ldh*::*ery*	(Hoefnagel et al., 2002a)
NZ9020	NZ9010 derivative, *ldh*::*ery*, *ldhB*::*tet*	(Bongers et al., 2003)

2.1.2 Plasmids

Table 2. *E. coli* plasmids used in this study.

Plasmid name	Characteristics	Source
pGEM-T Easy	Ap^r, T7 & SP6 RNA promoter, *lacZ*	Promega
pUC19	Ap^r	Invitrogen
pUC19_cm	Ap^r, cm^r	This Study
pGEM-T_eutD5'	Ap^r, T7 & SP6 RNA promoter, *lacZ*	This Study
pGEM-T_eutD3'	Ap^r, T7 & SP6 RNA promoter, *lacZ*	This Study
pGEM-T_eutD5'-eutD3'	Ap^r, T7 & SP6 RNA promoter, *lacZ*	This Study
pGEM-T_Ery^r	Ap^r; Ery^r, T7 & SP6 RNA promoter, *lacZ*	This Study
pGEM-T_eutD5'-Ery^r-eutD3'	Ap^r; Ery^r, T7 & SP6 RNA promoter, *lacZ*	This Study
pUC19_eutD5'-Ery^r-eutD3'	Ap^r, Cm^r, Ery^r	This study

pGEM-T_adhE5'	Ap^r, T7 & SP6 RNA promoter, *lacZ*	This Study
pGEM-T_adhE3'	Ap^r, T7 & SP6 RNA promoter, *lacZ*	This Study
pGEM-T_adhE5'-adhE3'	Ap^r, T7 & SP6 RNA promoter, *lacZ*	This Study
pGEM-T_Tet^r	Ap^r, T7 & SP6 RNA promoter, *lacZ*	This Study
pGEM-T_adhE5'-Tet^r-adhE3'	Ap^r, T7 & SP6 RNA promoter, *lacZ*	This Study
pUC19_adhE5'-Tc^r-adhE3'	Ap^r, Cm^r	This study
pGEM-T_eutD	Ap^r, T7 & SP6 RNA promoter, *lacZ*	This Study
pGEM-T_adhE	Ap^r, T7 & SP6 RNA promoter, *lacZ*	This Study

Table 3. *L. lactis* plasmids used in this study.

Plasmid name	Characteristics	Source
pNZ-8148	Cm^r; pSH71 origin, P_{nisA}	(Mifune et al., 2009)
pNZ-CAB	Cm^r; P_{nisA}-*phaCAB*	(Mifune et al., 2009)
pUC19_adhE5'-Tc^r-adhE3'	Cm^r, Tc^r	This study
pUC19_eutD5'-Ery^r-eutD3'	Cm^r, Ery^r	This study

2.2 Oligonucleotides

The following primers were used in this study.

Table 4. Primers used in this study

Primer name	Description/sequence 5' to 3'	Source
Sequencing primers		
T7	Forward primer, amplification of N-terminal region	Allan Wilson
	TAA TAC GAC TCA CTA TAG GG	Centre
SP6	Reverse primer, amplification of C-terminal region	Allan Wilson
	ATT TAG GTG ACA CTA TAG	Centre
M13	Forward primer, amplification of N-terminal region	Allan Wilson
	CCC AGT CAC GAC GTT GTA AAA CG	Centre
M13	Reverse primer, amplification of C-terminal region	Allan Wilson
	AGC GGA TAA CAA TTT CAC ACA GG	Centre
adhE seqF	Forward primer, amplification of N-terminal region	This study
	GGT CAA TGC CGC GCT TAA GTC	
adhE seqR	Reverse primer, amplification of C-terminal region	This study
	CAA GCG CGT GTG ACA TAG CAT C	

Tet Fwd	Forward primer, amplification of N-terminal region CTG CTG CAT TCC CTT CAC TGA	This study
Tet Rev	Reverse primer, amplification of C-terminal region GCA AAC TCA TTC CAG AAG CAA	This study
pUC Fwd	Forward primer, amplification of N-terminal region TGG GTG AGC AAA AAC AGG AAG	This study
pUC Rev	Reverse primer, amplification of C-terminal region GGT TTC TTA GAC GTC AGG TGG	This study
***adhE* PCR primers**		
adhE EF	Forward primer, amplification of *adhE* 5' region TAT A**GA ATT C**CT AAA AAA GCC GCT CCA GCT GCA A	This study
adhE BR	Reverse primer, amplification of *adhE* 5' region TTA A**GG ATC C**TT TTT GCT GCA TGG CTT GA	This study
adhE BF	Forward primer, amplification of *adhE* 3' region GGC TT**G GAT CC**C ATT ATG ACC CAG CGC ATC CAA CTA	This study
adhE ER	Reverse primer, amplification of *adhE* 3' region TGC **GGA ATT** CGG TTG ACG AGG ATT AGC AGG	This study
adhE EF2	Forward primer, amplification of *adhE* 5' region GGC T**GA ATT C**CG TTA ATG AAA CTG GCC GTG GAG	This study
adhE BR2	Reverse primer, amplification of *adhE* 5' region GAG A**GG ATC C**CC TTG CGC TTG CAT TTT AGC GAC	This study
adhE BF2	Forward primer, amplification of *adhE* 3' region GTT A**GG ATC C**GA CTC CAT TTG CGG TTA TCA CTG	This study
adhE ER2	Reverse primer, amplification of *adhE* 3' region GCT C**GA ATT C**CG TGG GTA AGG GGT ACG TTT AAC	This study
adhE fwd	Forward primer, amplification of N-terminal region encoding *adhE* GTC TGA AAC CCT TGC TTA TAA AGC GAT TTC	This study
adhE rev	Reverse primer, amplification of C-terminal region encoding *adhE* CTC TGT TGG GAA TAG AAG AAC CCC TAA TTT	This study
***eutD* PCR primers**		
eutD EF	Forward primer, amplification of *eutD* 5' region CTC G**GA ATT C**GA ATT CGC CGA GAT ATT GAG G	This study
eutD BR	Reverse primer, amplification of *eutD* 5' region TAA A**GG ATC C**CC TCT GGG TTA ATT CCA CGT	This study
eutD BF	Forward primer, amplification of *eutD* 3' region	This study

	TAT T**GG ATC C**AT TTG ATG CTG CCT TTG TTC C	
eutD ER	Reverse primer, amplification of *eutD* 3' region	This study
	AGT C**GA ATT C**CT GAA CCA GTT TGC ATG GAA A	
eutD NF	Forward primer, amplification of N-terminal region encoding *eutD*	This study
	CCG C**CC ATG G**TG AGA AAC TTG TAA CCG AGG G	
eutD SR	Reverse primer, amplification of C-terminal region encoding *eutD*	This study
	AGC G**GA GCT C**GC AAC AAA AAA AAT CCG CCT C	
eutD Fwd	Forward primer, amplification of N-terminal region encoding *eutD*	This study
	GAC GAG CGT TTG CGT GAC TTA ATG GAT ATC	
eutD Rev	Reverse primer, amplification of C-terminal region encoding *eutD*	This study
	GTC CCG CAA TCA TTG CTG CTG TAG ATA ATA	
Antibiotic resistance PCR primers		
Tet BF	Forward primer, amplification of N-terminal region encoding Tet^r	This study
	GGC G**GG ATC C**GC TTC ACA GAA ATT CTA GAA CA	
Tet BR	Reverse primer, amplification of C-terminal region encoding Tet^r	This study
	TAT T**GG ATC C**GT TAA TAC GTG AGC TCT GCG AGG C	
Ery BF	Forward primer, amplification of N-terminal region encoding Ery^r	This study
	GTA A**GG ATC C**AA CTG GTT TAA GCC GAC TGC	
Ery BR	Reverse primer, amplification of C-terminal region encoding Ery^r	This study
	GTA T**GG ATC C**GG AGG AAA AAA TAT GGG CAT	

2.3 Liquid media

The liquid media used during this study is listed below. All liquid medium was autoclaved at 121˚C for 20 minutes. Supplements were sterilised by autoclaving at 121˚C for 20 minutes or by filtration through a 0.22 µm filter, prior to addition to sterile medium.

2.3.1 Luria-Bertani (LB)-Medium

20 g of Luria-Bertani (LB) media (Invitrogen) was added per litre of H_2O.

2.3.2 M17 and GM17 medium

42.5 g of M17 media (Merck, Germany) was added per litre of H_2O. GM17 media was prepared by addition of 0.5% (w/v) glucose to M17 medium.

2.4 Solid media

15 g of agar (Oxoid) was added per litre of liquid media prior to autoclaving.

2.4.1 X-Gal Medium

The following supplements were added to sterile LB-agar medium:

	Stock solution	**Final concentration**
IPTG	1 M dissolved in Milli-Q water	1 mM
X-Gal	4% (w/v) dissolved in DMSO	0.004 %

If necessary, the relevant antibiotics were added (2.5). All solutions were sterilised by filtration through a 0.22 µm filter.

2.5 Antibiotic stock solutions and final concentrations

Antibiotic stock solutions were prepared according to Table 6. The stocks were sterilised by filtration through a 0.22 µm filter, aliquoted and stored at -20˚C for future use. When required, antibiotics were added at the concentrations given below (Table 6) to the nutrient media after autoclaving and when the media was cooled to 50˚C.

Table 5. Antibiotic stock solutions and concentrations.

Antibiotic	**Stock solution (mg mL^{-1}) and solvent**	**Final concentration (µg mL^{-1})**
For *E. coli*		
Ampicillin (sodium salt)	75 in H_2O	75
Chloramphenicol	5 in EtOH (absolute)	5
Tetracycline (hydrochloride)	12.5 in EtOH (70%)	12.5
Erythromycin	5 in H_2O	5
For *L. lactis*		
Chloramphenicol	10 in EtOH (absolute)	10
Erythromycin	5 in H_2O	5
Tetracycline	5 in EtOH (70%)	5
Nisin	0.25 in acetic acid (0.05 %)	0.01

2.6 Cultivation conditions

Liquid culture cultivations were performed in Erlenmeyer flasks with a flask volume: liquid volume ratio of approximately 3-5:1. Cultivations were performed in liquid LB media for *E. coli* or GM17 for *L. lactis*, with appropriate antibiotics. Flasks were incubated at 30˚C for *L. lactis* or 37˚C for *E. coli* XL1-Blue and Top10 with agitation on a gyratory shaker G-25 (New Brunswick Scientific, USA) or Thermoline orbital shaker TLMSIO (N.S.W, Australia), respectively, at approximately 200 rpm.

2.6.1 PHA accumulating conditions for *L. lactis*

L. lactis strains NZ9000, NZ9020 or NZ9000 Δ*eutD* containing either the pNZ-CAB or pNZ-8148 plasmid were used to inoculate GM17 medium containing appropriate antibiotics. This culture was left to grow overnight at 30˚C with agitation on a Thermoline orbital shaker TLMSIO (N.S.W, Australia) at approximately 200 rpm. 1% (v/v) of overnight culture was used to inoculate a large culture which was cultivated in M17 medium containing 1% (w/v) glucose, 0.3% (w/v) L-arginine and appropriate antibiotics, at 30˚C with agitation on a gyratory shaker G-25 (New Brunswick Scientific, USA). Once the OD_{600nm} of the culture reached 0.4-0.5, induction was performed by the addition of nisin (Sigma-Aldrich, USA) at a final concentration of 10 ng/mL. Cultures were grown at 30˚C with agitation on a gyratory shaker G-25 (New Brunswick Scientific, USA) for 24-48 hours.

2.7 Selection on solid media – Blue/white selection

The pGEM-T Easy vector system uses blue/white selection to differentiate between successful ligations of pGEM-T Easy vector and insert, and empty pGEM-T Easy vector. After ligation (2.11.8), the ligation mixture was transformed into *E. coli* (2.10.1) XL1-Blue (Invitrogen), plated out onto X-Gal plates (2.4.1) containing the appropriate antibiotics and incubated at 37˚C overnight. Blue colonies indicated no disruption of the β-galactosidase, whereas white colonies indicated inactivation of the β-galactosidase by successful ligation of insert. White colonies where therefore selected and streaked onto fresh X-Gal plates to confirm the loss of β-galactosidase activity

2.8 Storage of bacterial strains

2.8.1 Storage of *E. coli* strains

Recombinant *E. coli* strains were grown overnight in LB liquid media in the presence of appropriate antibiotics at 37˚C on a Thermoline orbital shaker TLM510 (N.S.W, Australia). 1 mL of the overnight culture was mixed with 70 µL of sterile dimethylsulfoxide (DMSO) giving a final concentration of 6.5% (v/v) in 2 mL cryovial tubes and stored at -80˚C.

2.8.2 Storage of *L. lactis* strains

Recombinant *L. Lactis* strains were grown overnight in GM17 liquid media in the presence of antibiotics at 30˚C on a gyratory shaker G-25 (New Brunswick Scientific, USA). 1.2 mL of the overnight culture was mixed with 400 µL of sterile 60% glycerol giving a final concentration of 15% (v/v) in 2 mL cryovial tubes and stored at -80˚C.

2.8.3 Strain revival

To revive the strain, 20 µL of the stock was added to 20 mL of liquid media (LB for *E. coli*; GM17 for *L. lactis*) containing the appropriate antibiotics in a 150 mL conical flask. Flasks were incubated at 37˚C for *E. coli* and 30˚C for *L. lactis* on a Thermoline orbital shaker TLM510 (N.S.W, Australia) or a gyratory shaker G-25 (New Brunswick Scientific, USA) respectively.

2.9 Preparation of competent cells

2.9.1 Competent *E. coli*

50 mL LB media was inoculated with 1% (v/v) of overnight culture and incubated at 37˚C until OD_{600} reached approximately 0.3. The culture was then incubated on ice for 15 min before centrifugation at 2250 x g in a Heraeus Multifuge 1 S-R, (Germany) to harvest the cells. The cells were resuspended in 16 mL RF1 solution before incubation on ice for 30 min and 15 min centrifugation at 2250 x g (Heraeus Multifuge 1 S-R Germany). The cells were resuspended in 4 mL RF2 solution and stored at -80˚C in 200 µL aliquots for future use.

RF1 solution

100 mM	RbCl
50 mM	$MnCl_2$
30 mM	Potassium acetate
10 mM	$CaCl_2.6H_2O$

Adjust the pH to 5.8 using acetic acid

RF2 solution

10 mM	RbCl
10 mM	MOPS
75 mM	$CaCl_2.6H_2O$
15 % (v/v)	Glycerol

Adjust the pH to 5.8 using NaOH

2.9.2 Electro-competent *L. lactis*

L. lactis was prepared according to protocol developed by NIZO Food Research (Netherlands). 20 mL of SGM17 (Gm17 supplemented with 0.2 M sucrose and 1% (w/v) glycine) containing the appropriate antibiotics was inoculated with 20 µL of *L. lactis* frozen stock and grown overnight at 30˚C on a gyratory shaker G-25 (New Brunswick Scientific, USA). 100 mL of SGM17 was then inoculated with 5% (v/v) of overnight culture and grown at 30˚C on a gyratory shaker G-25 (New Brunswick Scientific, USA) until the OD_{600nm} reached ~0.4. The culture was divided between two 50 mL falcon tubes (Greiner Bio-One) and centrifuged at 4,000 x g for 15 min (Heraeus multifuge1 S-R, Sorvall) to harvest the cells. The supernatant was discarded and each pellet re-suspended in 50 mL of ice cold 0.5 M sucrose containing 10% (v/v) glycerol, before centrifugation at 4,000 x g for 15 min (Heraeus multifuge1 S-R, Sorvall). The pellets were re-suspended in 25 mL of ice cold 0.5 M sucrose containing 10% (v/v) glycerol and 0.05% (w/v) EDTA and combined into one falcon tube to make a total of 50 mL. The cells were incubated on ice for 15 min before centrifugation at 4,000 x g for 15 min (Heraeus multifuge1 S-R, Sorvall), after which the supernatant was discarded and the cells again re-suspended in 50 mL of ice cold 0.5 M sucrose containing 10% (v/v) glycerol. Following another centrifugation step, the supernatant

was again discarded and the cells re-suspended in 1 mL ice cold 0.5 M sucrose containing 10% (v/v) glycerol. The cells were stored at -80˚C in 40 µL aliquots for future use.

2.10 Transformation and electroporation

2.10.1 Transformation of plasmid into *E. coli*

200 µL of competent *E. coli* cells from -80˚C were incubated on ice for 40 min before addition of 2 µL of plasmid DNA or 9 µL of ligation mix. The mixture was incubated on ice for a further 20 min to allow the DNA to adsorb to the surface of the cells. The cells were heat shocked at 42˚C for 90 sec allow uptake of the DNA, and then incubated on ice for 5 min. 800 µL of LB media was added and the cells incubated at 37˚C for 1 hr with shaking (Thermoline orbital shaker TLM510, N.S.W, Australia). To obtain single recombinant colonies, 100 µL was spread onto solid media plates containing the appropriate antibiotics. The remaining cells were centrifuged at 15,000 x g (Heraeus Multifuge 1 S-R Germany), resuspended in 100 µL fresh LB and plated onto solid media plates containing appropriate antibiotics. Plates were incubated at 37˚C overnight.

2.10.2 Electroporation of plasmid into *L. lactis*

40 µL of competent *L. lactis* cells from -80˚C were incubated on ice for 40 min before 2 µL of plasmid DNA was added and mixed with the cells. This mixture was transferred to an ice chilled 0.2 cm cuvette (Bio-Rad Laboratories, USA) and incubated on ice for a further 20 min. To electroporate the cells, a BIORAD MicroPulser (Bio-Rad Laboratories, USA) set at 2 kv and 1 pulse with a time constant of 5.8 ms was used to increase cell permeability of the plasma membrane. Immediately after electroporation, 1 mL of sterile recovery medium (GM17 supplemented with 20 mM $MgCl_2$ and 2 mM $CaCl_2$) was added and the mixture transferred to a 1.5 mL microfuge tube on ice. The cells were incubated on ice for 10 min before being further incubated for 2-3 hours at 30˚C with agitation on a gyratory shaker G-25 (New Brunswick Scientific, USA). To obtain single recombinant colonies, 100 µL was spread onto solid GM17 media plates containing the appropriate antibiotics. The remaining cells were centrifuged at 15,000 x g (Heraeus Multifuge 1 S-R Germany), resuspended in 100 µL fresh GM17 and plated

onto solid GM17 media plates containing appropriate antibiotics. Plates were incubated at 30˚C for 48 hr.

2.11 DNA manipulation

2.11.1 Plasmid isolation and concentration

Plasmid isolation from recombinant *E. coli* was done by one of two methods described below:

2.11.1.1 Fast plasmid mini-prep

E. coli strains containing the relevant plasmid were incubated in 10 mL LB media with the appropriate antibiotics at 37˚C overnight. 1.5 mL of overnight culture was centrifuged for 1 min at 15,000 x g (biofuge Pico, Heraeus, Germany), and most of the supernatant removed leaving 50-100 µL in which the pellet was resuspended. This was followed by the addition of 300 µL TENS buffer. The tube was vortexed for approximately 10 seconds before being incubated on ice for 10 min. To precipitate the protein, 150 µL sodium acetate (pH5.2) was added and the tube vortexed for ~10 seconds. After centrifugation at 15,000 x g for 10 min, the supernatant was transferred to a fresh microfuge tube containing 900 µL 100% ethanol precooled to -20˚C, and centrifuged at 15,000 x g for 2 min. The supernatant was removed and 1 mL of 70% ethanol added. The pellet was resuspended by vortexing and the tube centrifuged at 10,000 x g for a further 10 min. The supernatant was removed and the tube left to dry completely at room temperature. Once dry, the isolated plasmid DNA was dissolved in 30 µL of TER buffer and stored at -20˚C.

TENS buffer

10 mM	Tris-HCl (pH 8.0)
1 mM	EDTA
0.5% (w/v)	SDS
0.1 M	NaOH

RNase solution: to make TER buffer

150 mM	NaCl
1% (w/v)	RNase A

TE buffer: to make TER buffer

10 mM	TrisHCl (pH 8.0)
1 mM	EDTA

TER buffer

10 µL RNase solution: 990 µL TE buffer

2.11.1.2 High Pure Plasmid isolation kit

Plasmid isolation using the High Pure Plasmid isolation kit (Roche, Switzerland) was performed according to manufacturer's instructions.

2.11.1.3 Plasmid isolation from *L. lactis*

L. lactis strains containing the relevant plasmid were incubated in 10 mL GM17 media with the appropriate antibiotics at 30˚C overnight. 1.5 mL of overnight culture was centrifuged for 1 min at 15,000 x g (Heraeus Pico 17, Thermo Scientific, Germany). The supernatant was poured off and the centrifugation step repeated twice. The supernatant was removed, the pellet was resuspended in 250 µL THMS-buffer containing 10 mg/mL lysozyme and the tube incubated at 37˚C for 10-15 min. Cells were lysed by the addition of 500 µL lysis buffer (0.2 N NaOH + 3% SDS), gentle inversion a few times and incubation on ice for 5 min. Following cell lysis, the remaining steps to isolate the plasmid were performed using the Roche High Pure Plasmid Isolation Kit according to the manufacturer's instructions.

THMS-buffer

30 mM	TrisHCl (pH 8.0)
3 mM	$MgCl_2$
25% (w/v)	Sucrose

2.11.2 Genomic DNA isolation from *L. lactis*

Genomic DNA isolation from *L. lactis* was performed using the GenElute Bacterial Genomic DNA kit (Sigma-Aldrich) according to manufacturer's instructions for Gram-positive organisms.

2.11.3 Clean and Concentrator kit

The Clean and Concentrator kit (Zymo Research, USA) was used following the manufacturer's instructions to concentrate or clean DNA samples as required.

2.11.4 Determination of DNA concentration

For determination of DNA concentration, the Qubit$_{TM}$ fluorometer (Invitrogen, USA) was used in combination with the Quant-iT DNA BR assay kit (Invitrogen, USA) according to the manufacturer's instructions.

2.11.5 DNA hydrolysis with restriction endonucleases

All restriction enzymes were purchased commercially from Invitrogen, Roche or New England Biolabs and were used according to the manufacturer's instructions. DNA hydrolysis using restriction enzymes was used for restriction analysis of DNA and for cloning purposes. When two or more restriction enzymes with compatible buffers were used, they were combined into a single reaction; when the buffers were incombatible, an intermediate ispropanol precipitation step was required (2.11.5.1).

2.11.5.1 Iso-propanol precipitation of DNA

3 volumes of iso-propanol was added, and the tube was incubated on ice for 5 min to precipitate the DNA. After centrifugation at 16,200 x g for 30 min (Heraeus Pico 17, Thermo Scientific) to sediment the DNA, the supernatant was carefully removed and

the sediment washed once with 3 volumes of 70% ethanol to remove traces of iso-propanol. The tube was centrifuged as before, the ethanol removed and the tube left to dry at room temperature.

2.11.6 Agarose gel electrophoresis (AGE)

Agarose gel electrophoresis was performed using horizontal gel slabs to separate DNA fragments. 1-2% agarose in 1 x TBE buffer was used; 1% for fragments >1000 bp, 2% for fragments <1000 bp. A suitable molecular size standard and the DNA samples were loaded into the wells of the gel after the addition of 3 x loading dye to each sample. The electrophoresis conditions were 100-120 V for 35 – 60 min using a Biometra gel electrophoresis unit (Biometra, Germany). After electrophoresis, the gel was stained in ethidium bromide solution at a concentration of 10 µg/mL for approximately 20 min, soaked in water for 10 min and then visualised using a UV transilluminator at λ = 254 nm (Bio-Rad, Gel Doc 2000).

For DNA fragments that needed to be recovered from agarose gels, SYBR Safe DNA gel stain was used instead of EtBr according to the manufacturer's instructions and visualised using a blue light screen (Invitrogen, USA).

1x TBE

50 mM	Tris-HCl
50 mM	Boric acid
2.5 mM	EDTA

Adjust to pH 8.0 using HCl

3x Loading dye

60 mM	Tris-HCl
60 mM	EDTA
60% (v/v)	Glycerol
0.2% (w/v)	Orange G
0.05% (w/v)	Xylene Cyanol FF

2.11.6.1 DNA molecular size standards

The size of DNA fragments was estimated by comparison with fragments of a known size. Typically λ-DNA (Invitrogen, USA) digested with *Pst*I restriction endonuclease was used.

2.11.7 Agarose gel DNA fragment recovery

For the recovery of DNA fragments from AGE (2.11.6), QIAquick® Gel Extraction Kit (Qiagen, Germany) was used according to manufacturer's instructions.

2.11.8 DNA A-tailing and ligation (pGEM-T Easy system)

To efficiently ligate blunt-end PCR products into the pGEM-T Easy cloning vector, the fragments needed to be A-tailed. A typical 10 µL A-tailing reaction mixture contained the following:

A-tailing reaction mix

1 µL	dATP (0.2 mM)
1 µL	*Taq*-DNA polymerase (Invitrogen)
1 µL	10x *Taq* reaction buffer (-$MgCl_2$)
1 µL	$MgCl_2$
6 µL	PCR product

The reaction mixture was incubated at 70˚C for 30 min. 3.5 µL of the A-tailed product was used in a ligation mixture containing the following:

pGEM-T Easy ligation mix

5 µL	pGEM-T Easy 2x ligase buffer
0.5 µL	pGEM-T Easy vector
1 µl	pGEM-T Easy ligase
3.5 µL	A-tailed PCR product

The reaction mixture was incubated at 4˚C in a floating waterbath overnight.

2.11.9 DNA ligation (T4 DNA ligase)

For the ligation of fragments into appropriate expression vectors, the fragments were first generated by DNA hydrolysis using the appropriate restriction endonuclease and then separated and isolated using AGE (2.11.6). Reactions were set up in 700 µL microfuge tubes with a high insert to vector ratio (≥ 6:1) and according to the manufacturer's instructions for T4 DNA ligase (Invitrogen, USA). Tubes were incubated at 4˚C in a floating water bath overnight.

2.11.9.1 Dephosphorylation of 5' ends

For the de-phosphorylation of vectors to prevent re-ligation, digested vector was treated with Antarctic phosphatase (Invitrogen) according to the manufacturer's instructions prior to ligation.

2.11.10 Polymerase Chain Reaction (PCR)

Polymerase chain reaction (PCR) was performed for the amplification of DNA fragments from template DNA. Specific oligonucleotide primers were used to flank the target fragment on the template DNA. PCR reactions were performed in a Biometra T Personal Thermocycler (Whatman Biometra, Germany) using repeated cycles of denaturation, annealing and extension. Platinum *Pfx* DNA polymerase (Invitrogen, USA) was used when high fidelity was required and a slightly modified version of the manufacturer's instructions followed. A typical reaction mixture is listed below.

PCR reaction mix

In 100 µL total volume	Final Concentration
10 µL 10 X *Pfx* amplification buffer	1 x
5 µL $MgSO_4$ (50mM)	2.5 mM
5 µL DMSO	5%
10 µL forward primer	0.1 µM
10 µL reverse primer	0.1 µM
10 µL dNTPs (mixture of dATP, dTTP, dCTP and dGTP*)	0.1 mM of each
~1 - 10 ng Template DNA	
0.5 µL *Pfx*-DNA-polymerase	1 unit
to 100 µL autoclaved distilled H_2O	
*(Roche NZ Ltd)	

2.11.11 DNA sequencing

All sequencing of PCR products or recombinant plasmids was carried out by the Allan Wilson Centre Genome Service using a capillary ABI3730 Genetic Analyzer (Applied Biosystems Inc). Each sequencing reaction was set up in a sterile 0.2 mL thin walled PCR tube (Axygen, USA) and containing 3.2 pmol of primer and ~300 ng of DNA in 15 µL. Results were provided in ABI format and analysed using Vector NTI version 11.

2.12 Gas chromatography-mass spectrometry analysis (GC/MS)

15 mg of lyophilised cells were suspended in 2 mL of chloroform and subjected to methanolysis by the addition of 2 mL methanol in the presence of 15% (v/v) sulphuric acid. Methanolysis was performed by incubating the tubes in an oil bath heated to 100˚C for 5 hours before being removed and left to cool to room temperature. Once cool, 2 mL of water was added and the tubes vortexed thoroughly for approximately 30 seconds before being left at room temperature for the phases to separate. The bottom phase containing methyl esters of the corresponding fatty acid constituents was removed and sent for analysis by gas chromatography-mass spectrometry (GC/MS) at Plant and Food (Palmerston North).

2.13 Analysis of lactate and acetate

L. lactis strains were grown over a 24 hr period under PHA accumulating conditions as described in section 2.6.1. At specified time intervals, samples were taken from the cultures, centrifuged to remove the cells and the supernatant stored at -80˚C for later analysis. The concentration of lactate and acetate in the culture supernatant was measured using the L-Lactic Acid kit (Megazyme, Ireland; 2.13.1) or Acetic Acid kit (Acetate Kinase Format; Megazyme, Ireland; 2.13.2).

2.13.1 Lactate assay

Quantification of lactate was performed using the K-LATE L-Lactic Acid assay kit (Megazyme, Ireland) according to the maufacturer's instructions for a 96-well microplate format (LATE-MPF). 132 µL of autoclaved distilled water was added to the well along with 10 µL sample, 50 µL solution 1 (buffer), 10 µL solution 2 (NAD^+) and 10 µL suspension 3 (D-GTP diluted 1:5). The sample was mixed, incubated ~3 min, and read at λ = 340 nm (A1) on an ELx808iu ultra microplate reader (BIO-TEK Instruments Inc., USA). After the initial reading, 10 µL of suspension 4 (L-LDH diluted 1:5) was added to the well to initiate the reaction, the sample was mixed and after incubation at 25˚C for 10 min, the sample was read at λ = 340 nm (A2). The absorbance at 340 nm was then read every 5 min until the absorbances either remained the same. To calculate the change in absorbance, the final A2 reading was subtracted from the A1 reading. This value was then compared with the standard curve of known lactate concentrations (made from the L-Lactic acid standard solution provided) to calculate the concentration in the test samples.

2.13.2 Acetate assay

Quantification of acetate was performed using the K-ACETAK Acetic Acid assay kit (Megazyme, Ireland) and was used according to the maufacturer's instructions using a 96 well format. 290 µL of R1 was added to the well along with 5 µL sample. The sample was mixed and read at λ = 340 nm (A1) on an ELx808iu ultra microplate reader (BIO-TEK Instruments Inc., USA). After the initial reading, 20 µL of R2 was added to the well to initiate the reaction, the sample was mixed and after incubation at 37˚C for 10 min, the sample was read at λ = 340 nm (A2). To calculate the change in absorbance, the final A2 reading was subtracted from the A1 reading. This value was then compared

with the standard curve of known acetate concentrations (made using 100 % acetic acid and Milli-Q water to concentrations ranging from 5 to 30 μg/mL) to calculate the concentration in the test samples.

CHAPTER 3: RESULTS

There are two parts to the results. The first involves the construction of the *L. lactis* NZ9000 Δ*eutD* strain and subsequent analysis. The second involves the attempted construction of an *L. lactis* NZ9000 Δ*adhE* strain.

Part I: NZ9000 Δ*eutD*

3.1 Construction of an *eutD* knockout plasmid

To construct an *eutD*::*ery* replacement strain of *L. lactis* NZ9000, a plasmid was constructed that allowed selection of the desired mutant through a double cross-over event on both flanking regions of the *eutD* gene. Plasmid pUC_*eutD*5'_Ery^R_*eutD*3' was constructed to contain both a 5' fragment and a 3' fragment on the *eutD* gene, with an internal erythromycin resistance cassette. Construction of this plasmid was a multi step process (Figures 5 & 6).

First, primers were designed to amplify a 625 bp fragment containing a 5' section of the *eutD* gene and a 508 bp fragment containing a 3' section of the *eutD* gene (Table 4). These primers were used in PCR reactions (2.11.10) with linearized NZ9000 *L. lactis* genomic DNA as a template. Primers were also designed to amplify an erythromycin resistance gene from the pE194 plasmid (Maguin et al., 1996). These primers were used in a PCR reaction with whole plasmid as a template. PCR-generated fragments of the correct sizes (625 bp for *eutD*5'; 508 bp for *eutD*3'; 1101 bp for Ery^R; results not shown) were isolated using AGE with SYBR Safe stain (2.11.6) and gel purified (2.11.7).

The second step involved cloning the fragments into the pGEM-T Easy vector system to allow for the fragments to be sequenced. After ligation into pGEM-T Easy (2.11.8), the products were transformed into *E. coli* XL1-Blue (2.10.1) and plated onto LB agar plates containing 0.004% X-gal, 1 mM IPTG, 12.5 µg/mL tetracycline and 75 µg/mL ampicillin (pGEM-T Easy_Ery transformation also contained 5 µg/mL erythromycin; 2.4.1). Single white colonies were isolated and cultured for plasmid isolation (2.11.1) and RE analysis (*Eco*RI for *eutD* fragments; *Bam*HI for EryR; 2.11.5). After complete digestion, AGE was used to visualise the fragments (2.11.6): two fragments of expected

size 625 bp and 2997 bp were seen for *eutD*5'; two fragments of expected size 508 bp and 2997 bp were seen for *eutD*3'; and two fragments of expected size 1101 bp and 3030 bp were seen for Ery^R (results not shown). Plasmids displaying the correct band pattern were sent for sequence analysis (2.11.11).

Once all fragments had been confirmed by sequencing, they were ligated together into one pGEM-T Easy vector. Firstly the pGEM-T Easy vector was linearised by RE analysis using *Eco*RI (2.11.5), isolated and purified from an agarose gel (2.11.7) and treated with Antarctic phosphatase to prevent religation of the vector (2.11.9.1). The *eutD*5' and *eutD*3' fragments were excised from the pGEM-T Easy eutD5' and eutD3' vectors by RE digest using *Eco*RI and *Bam*HI, isolated and purified from agarose gel using gel purification. The *eutD*5' and *eutD*3' fragments were then ligated into the *Eco*RI site of the pGEM-T Easy vector using T4 DNA ligase (2.11.9). The ligation product was transformed into *E. coli* XL1-Blue (2.10.1) and plated onto LB agar containing 4% X-gal, 1 mM IPTG, 12.5 µg/mL tetracycline and 75 µg/mL ampicillin (2.4.1). Single white colonies were isolated and cultured for plasmid isolation (2.11.1) and RE analysis using *Eco*RI (2.11.5); two fragments of expected size 1106 bp and 2997 bp were seen after complete digestion using AGE (2.11.6; results not shown). Plasmid displaying the correct restriction pattern was isolated and linearised by RE digest using *BamH*I, gel-purified (2.11.6-7) and treated with Antarctic phosphatase to prevent religation of the vector (2.11.9.1). The Ery^R gene was excised from the pGEM-T Easy_EryR vector by RE digest using *Bam*HI and gel-purified (2.11.6-7). The Ery^R gene was then ligated into the *Bam*HI site of the pGEM-T Easy_*eutD*5'_*eutD*3' vector using T4 DNA ligase (2.11.9). The ligation product was transformed into *E. coli* XL1-Blue (2.10.1) and plated onto LB agar containing 4% X-gal, 1 mM IPTG, 12.5 µg/mL tetracycline, 75 µg/mL ampicillin and 5 µg/mL erythromycin (2.4.1). Single white colonies were selected for plasmid isolation (2.11.1) and RE analysis using *Eco*RI (2.11.5); two fragments of expected size 2207 bp and 2997 bp were seen after complete digestion using AGE (2.11.6; results not shown).

pUC19 was chosen as the plasmid to use for the integration of the resistance cassette into the target gene as it is a high copy number plasmid that is very easy to work with in *E. coli* yet cannot propagate in *L. lactis*. An additional resistance gene outside of the recombination site was required so that selective plating could be used to differentiate

between colonies that had undergone a single cross-over and those that had undergone a double cross-over. The chloramphenicol resistance gene from the pNZ-8148 plasmid was excised using *Ssp*I (2.11.5), separated using AGE with SYBR safe stain (2.11.6), and gel purified (2.11.7). The chloramphenicol gene was then ligated into the *Ssp*I site of the linearized pUC19 vector using T4 DNA ligase (2.11.9). The product was transformed into *E. coli* XL1-Blue (2.10.1) and plated onto LB agar containing 12.5 µg/mL tetracycline, 75 µg/mL ampicillin and 5 µg/mL chloramphenicol (2.5). Single white colonies were isolated and cultured for plasmid isolation and RE analysis using *Ssp*I; two fragments of expected size 927 bp and 2686 bp were seen using AGE (2.11.6; results not shown). The plasmid was also confirmed by sequencing (2.11.11).

The final step in constructing pUC_*eutD*5'_Ery^R_*eutD*3' involved excising the *eutD*5'_Ery^R_*eutD*3' fragment from pGEM-T Easy_eutD5'-EryR-eutD3' by RE digest using *Eco*RI (2.11.5). The fragment was separated using AGE with SYBR safe stain (2.11.6), isolated and gel-purified (2.11.7). The fragment was then ligated into the *Eco*RI site of the linearised pUC19_cm^R vector (2.11.9). The ligation product was transformed into *E. coli* XL1-Blue (2.10.1) and plated onto LB agar containing 12.5 µg/mL tetracycline, 5 µg/mL erythromycin and 5 µg/mL chloramphenicol. Single colonies were selected for plasmid isolation (2.11.1) and RE analysis using *Bgl*I (2.11.5); two fragments of expected size 2044 bp and 3663 bp were seen using AGE (2.11.6; Figure 4).

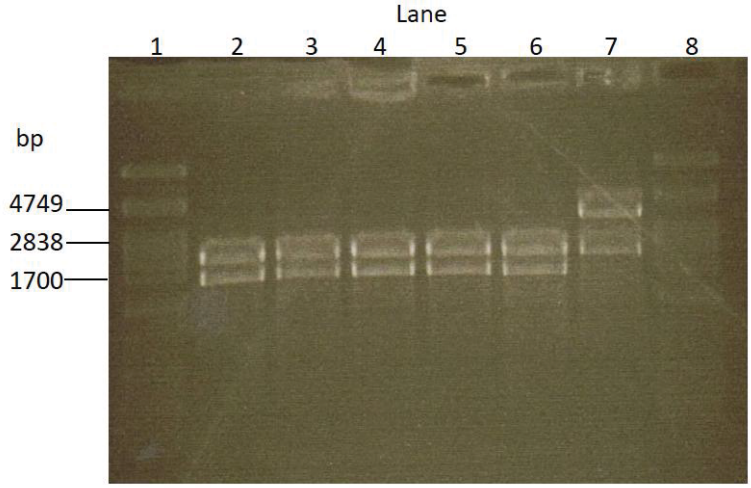

Figure 4. Restriction analysis of plasmid isolated from *E. coli* XL1-Blue cells transformed with pUC_*eutD*5'_Ery^R_*eutD*3'. Lanes 1 & 8, DNA ladder standard (λ *Pst*I); Lanes 2 – 7, isolated plasmid digested with *Bgl*I with expected sizes of 2044 bp and 3663 bp (complete digestion). Plasmid containing no insert runs at the expected size of 1456 bp and 2044 bp.

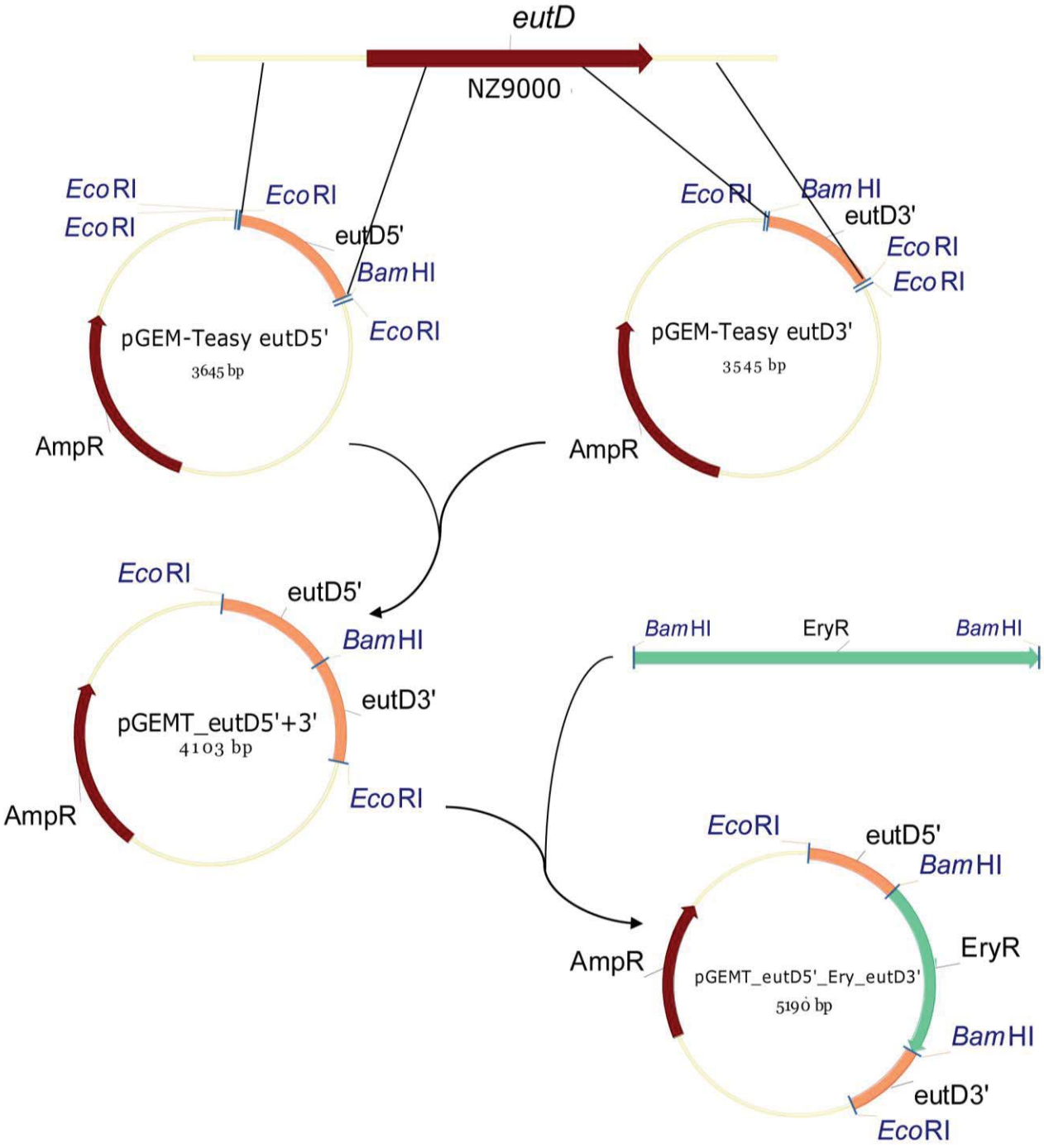

Figure 5. Construction of the intermediate cloning plasmid pGEMT_eutD5'_Ery^r_eutD3' for generation of pUC19_ eutD5'_Ery^r_eutD3'. The PCR fragments *eutD*5' and *eutD*3' were generated using primers eutD EF (forward) & eutD BR (reverse), and eutD BF (forward) and eutD ER (reverse), respectively. *Bsm*AI digested *L. lactis* NZ9000 genomic DNA was used as a template. The resulting 625 bp (*eutD*5') and 508 bp (*eutD*3') fragments were A-tailed and ligated into intermediate cloning vector pGEM-T Easy. Both fragments were then excised using *Eco*RI and ligated together into the similarly digested intermediate cloning vector pGEM-T Easy. The PCR fragment Ery^R was generated using primers Ery BF (forward) and Ery BR (reverse) using plasmid pE194 as a template. The resulting 1101 bp PCR product was ligated into the *Bam*HI site of the pGEMT_eutD5'_eutD3' plasmid. pGEMT_adhE5'_Tet^r_adhE3' was similarly constructed using primers adhE EF (forward) & adhE BR (reverse), and adhE BF (forward) and adhE ER (reverse) to generate PCR fragments *adhE*5' and *adhE*3', respectively. The PCR fragment Tet^r was generated using primers Tet BF (forward) and Tet BR (reverse) using plasmid pT181 as a template.

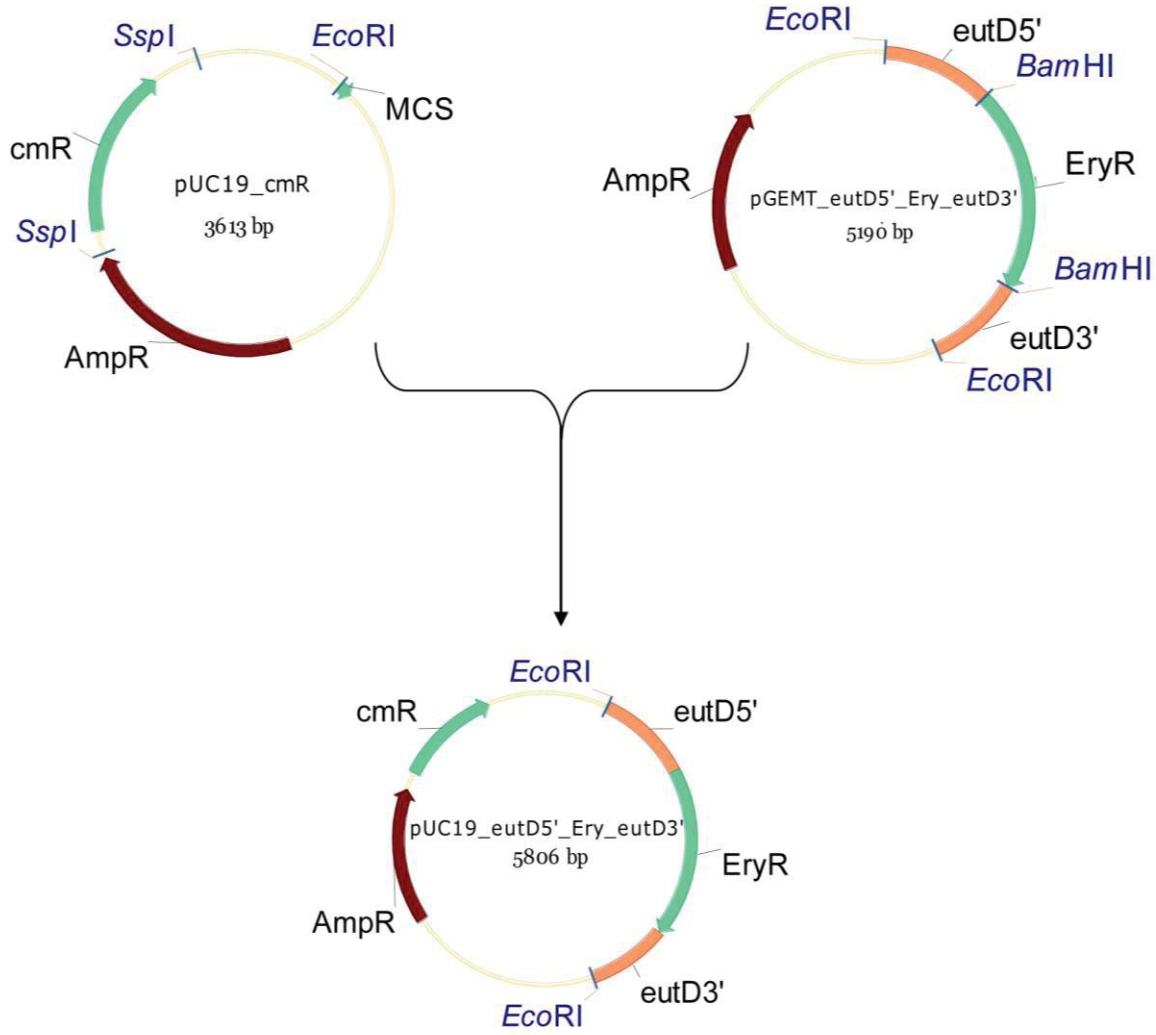

Figure 6. Construction of pUC19_eutD5'_Ery^r_eutD3'. The intermediate plasmid pGEMT_eutD5'_Ery^r_eutD3' was digested with *Eco*RI. The resulting 2207 bp fragment was ligated into *Eco*RI digested pUC19_cm^r using T4 DNA ligase. pUC19_adhE5'_Tet^r_adhE3' was similarly constructed from intermediate plasmid pGEMT_adhE5'_Tet^r_adhE3'.

3.2 Construction of the NZ9000 Δ*eutD* mutant

The first step in constructing the *L.* lactis NZ9000 *eutD* knockout strain was electroporation of pUC_*eutD*5'_Ery^{R}_*eutD*3' into NZ9000 (Figure 7; 2.10.2). After electroporation, the *L. lactis* cells were plated onto solid GM17 agar containing 1 µg/mL erythromycin (2.4). Single colonies were selected and plated onto fresh GM17 agar containing either 5 µg/mL erythromycin or 5 µg/mL erythromycin and 10 µg/mL chloramphenicol. Colonies that grew on the erythromycin plates but did not grow on the erythromycin and chloramphenicol plates were selected and cultured in liquid GM17 media containing 5 µg/mL erythromycin (2.3.2). Colonies that displayed erythromycin resistance and chloramphenicol sensitivity likely resulted from a one-step double cross-over event on both flanking regions of the *eutD* gene and thus should have the *eutD*:ery*t* replacement mutation. After overnight cultivation, the genomic DNA was isolated from the cells (2.11.2) and linearized by digestion with *Bsm*AI (2.11.5). The linearized DNA was then subjected to PCR (2.11.10) using primers targeting regions outside of the *eutD* recombination sites (Table 4). Wild type NZ9000 DNA was also linearized by digestion with *Bsm*AI and subjected to the same PCR cycle as a control. All fragments generated from the PCR reactions were then separated using AGE and SYBR safe stain (Figure 8; 2.11.6); fragments of the expected size (2241 bp) were isolated and gel-purified (2.11.7). These fragments were then subjected to RE analysis with *Bam*HI to confirm that the targeted *eutD* gene had been disrupted; bands present at 586 bp, 666 bp and 989 bp confirmed this (Figure 9).

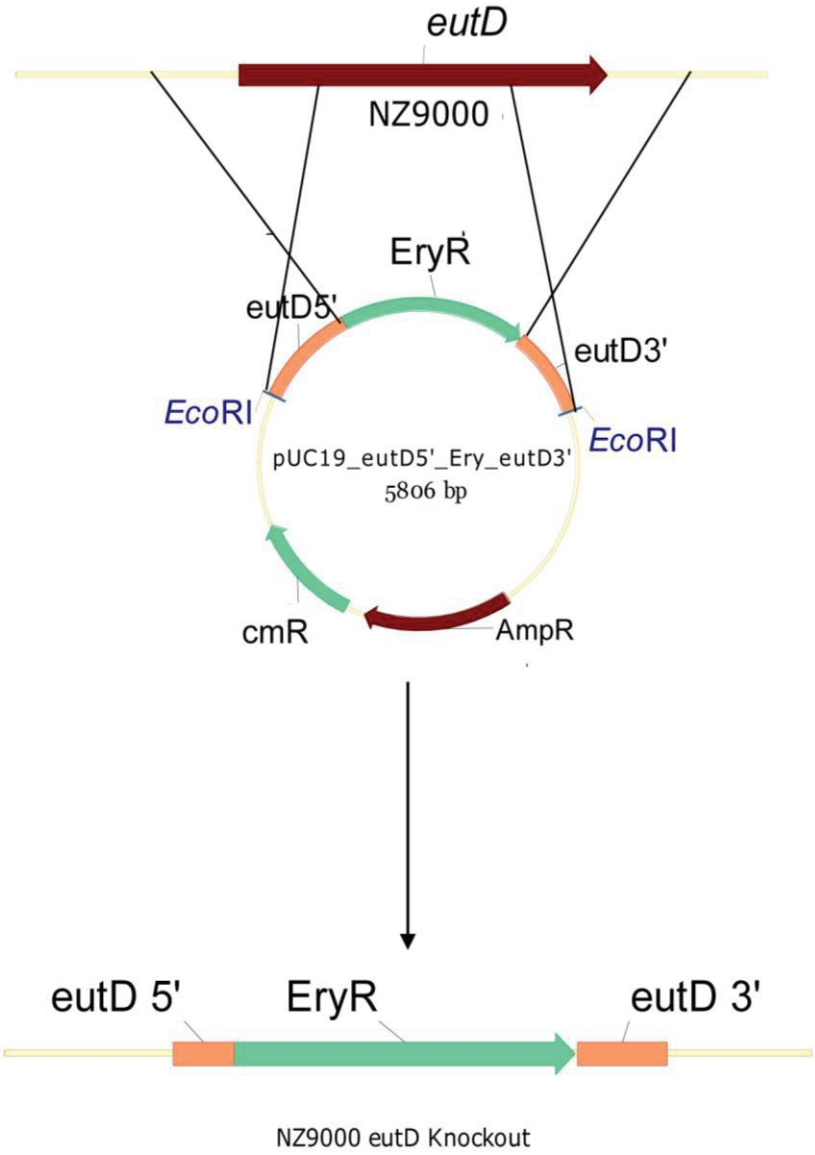

Figure 7. NZ9000 *eutD* knockout strategy. The suicide plasmid pUC19_eutD5'_Ery^r_eutD3' was electroporated into *L. lactis* NZ9000. A double cross-over event occurs on both homologous regions of the plasmid, incorporating the Ery^r cassette into the genome and disrupting the *eutD* gene. The suicide plasmid cannot propagate and is dropped by the strain. The same strategy was used to knockout the *adhE* gene using plasmid pUC19_adhE5'_Tet^r_adhE3'.

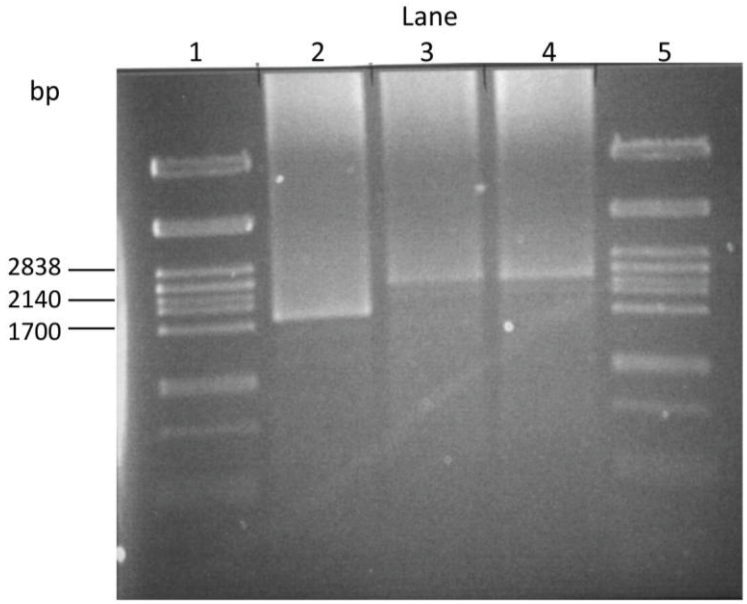

Figure 8. PCR analysis of NZ9000 and NZ9000 Δ*eutD* genomic DNA. Lanes 1 & 5, DNA ladder standard (λ *Pst*I); Lane 2, NZ9000 PCR with expected size 1787 bp; Lanes 3 & 4, NZ9000 Δ*eutD* PCR with expected size 2241 bp.

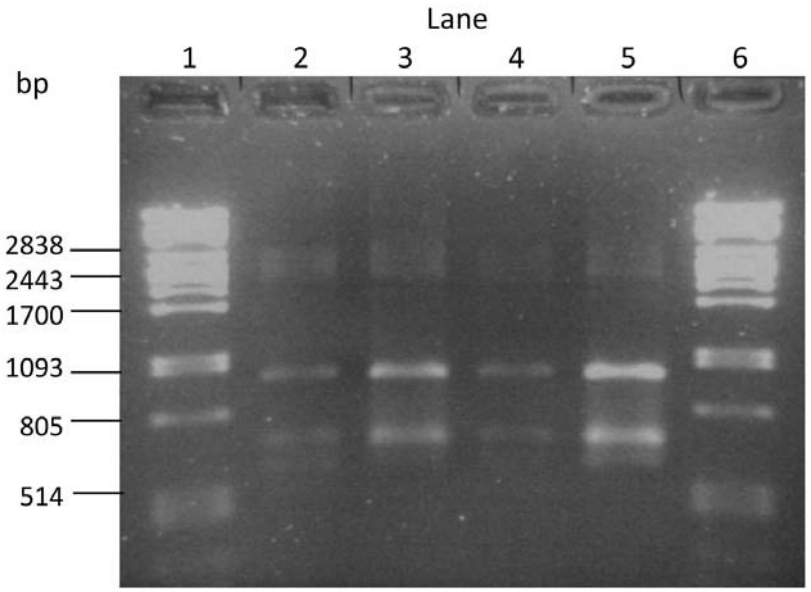

Figure 9. Restriction analysis of PCR-generated fragments from NZ9000 Δ*eutD* mutants. Lanes 1 & 6, DNA ladder standard (λ *Pst*I); Lanes 2 – 5, NZ9000 Δ*eutD* PCR fragments digested with *Bam*HI with expected sizes of 586 bp, 666 bp and 989 bp (complete digestion). The undigested DNA fragment runs at the expected size of 2241 bp. Partially digested DNA fragments run at 1575 bp and 1655 bp.

3.3 Phenotypic characterisation of NZ9000 Δ*eutD* mutant

To characterise the effects of knocking out the phosphate acetyltransferase pathway on PHB yield and the metabolic byproducts, the *eutD* knockout strain NZ9000 Δ*eutD* and positive control strain NZ9000 were electroporated with the plasmids pNZ-CAB and pNZ-8148 ((Mifune et al., 2009); 2.10.2). pNZ-CAB habours the codon optimized *phaCAB* operon from *Cupriavidus necator* allowing PHB production and pNZ-8148 is an empty-vector negative control. Transformants were plated onto GM17 agar plates containing 10 μg/mL chloramphenicol and single colonies were selected for plasmid isolation (2.11.1.3) and RE analysis using *Ssp*I for pNZ-8148 and *Nde*I for pNZ-CAB (2.4.1). After complete digestion, AGE was used to visualise the fragments (2.11.6): three fragments of expected size 730 bp, 927 bp and 1508 bp for pNZ-8148 (Figure 10), and four fragments of expected size 1103 bp, 1182 bp, 1352 bp and 3242 bp for pNZ-CAB (Figure 11) were seen, confirming that the transformation was successful.

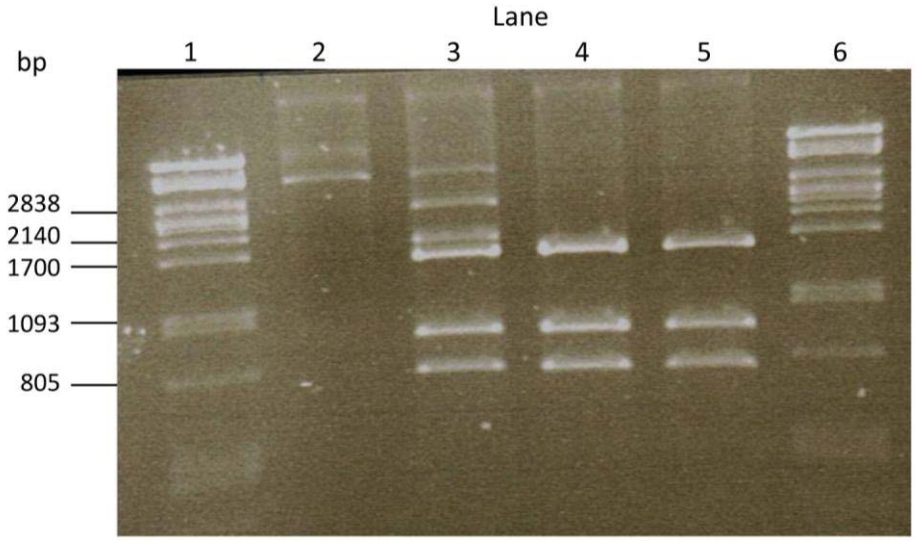

Figure 10. Restriction analysis of plasmid isolated from NZ9000 Δ*eutD* mutants electroporated with pNZ-8148. Lanes 1 & 6, DNA ladder standard (λ *Pst*I); Lanes 2 – 4, plasmid isolated from NZ9000 Δ*eutD* digested with *Ssp*I with expected sizes of 730 bp, 927 bp and 1508 bp (complete digestion); Lane 5, pNZ-8148 plasmid digested with *Ssp*I with expected sizes of 730 bp, 927 bp and 1508 bp (complete digestion). The linear plasmid runs at the expected size of 3165 bp; partially digested plasmid runs at 1657 bp, 2238 bp and 2435 bp.

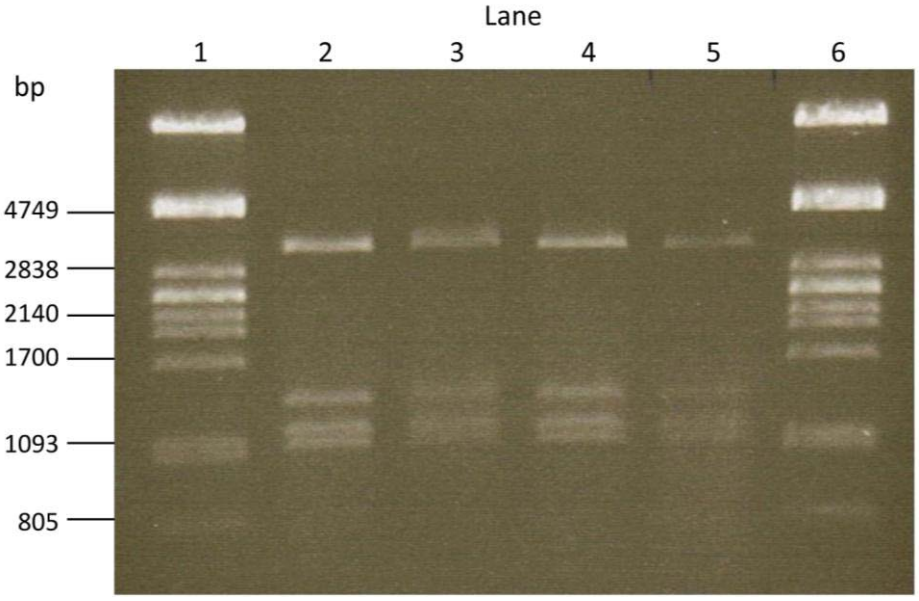

Figure 11. Restriction analysis of plasmid isolated from NZ9000 Δ*eutD* mutants electroporated with pNZ-CAB. Lanes 1 & 6, DNA ladder standard (λ *Pst*I); Lanes 2 – 4, plasmid isolated from NZ9000 Δ*eutD* digested with *Ssp*I with expected sizes of 1103 bp, 1182 bp, 1352 bp and 3242 bp (complete digestion). Lane 5, pNZ-CAB plasmid digested with *Ssp*I with expected sizes of 1103 bp, 1182 bp, 1352 bp and 3242 bp (complete digestion).

3.3.1 Growth and pH analysis of recombinant *L. lactis*

The first step in characterising a mutant strain is to determine how the mutation affects growth. *L. lactis* NZ9000, NZ9020 and NZ9000 Δ*eutD* strains harbouring either the pNZ-CAB or pNZ-8148 plasmids were grown for 24 hrs under PHB accumulating conditions in the presence of 10 µg/mL chloramphenicol for all strains, as well as an additional 5 µg/mL tetracycline for NZ9020 and 5 µg/mL erythromycin for NZ9000 Δ*eutD* (2.6.1). NZ9000 and NZ9020 were used as control strains. All experiments were performed in triplicate.

The NZ9000 WT control strain showed no significant differences between the pNZ-CAB plasmid and the pNZ-8148 plasmid, with both conditions giving comparable lag phases, growth rates and maximum optical cell densities (Figure 12). The NZ9020 strain showed a slightly longer lag phase when harbouring the pNZ-CAB plasmid (approximately 10 hrs) than when harbouring the pNZ-8148 plasmid (approximately 5 hrs); however the maximum cell density (OD_{600}) reached around 6 for both – consistently higher than the control (~4.8). The NZ9000 Δ*eutD* strain showed a considerably longer lag phase when compared to the NZ9000 WT control strain for both

plasmids and also had a considerably slower growth rate during log phase. The NZ9000 Δ*eutD* strain was the only strain where the maximum cell density was significantly affected by the harboured plasmid; when harbouring the pNZ-CAB plasmid the culture reached a cell density of approximately 5 compared with only 3.2 when harbouring the pNZ-8148 plasmid. As expected, the pH for the NZ9020 strain did not change significantly, only dropping from ~8 to ~7 indicating a reduced production of lactate. The pH of the NZ9000 and NZ9000 Δ*eutD* media had a much more siginificant drop from ~8 to ~5.5. No difference was seen in media pH between strains harbouring the pNZ-8148 plasmid and those harbouring pNZ-CAB.

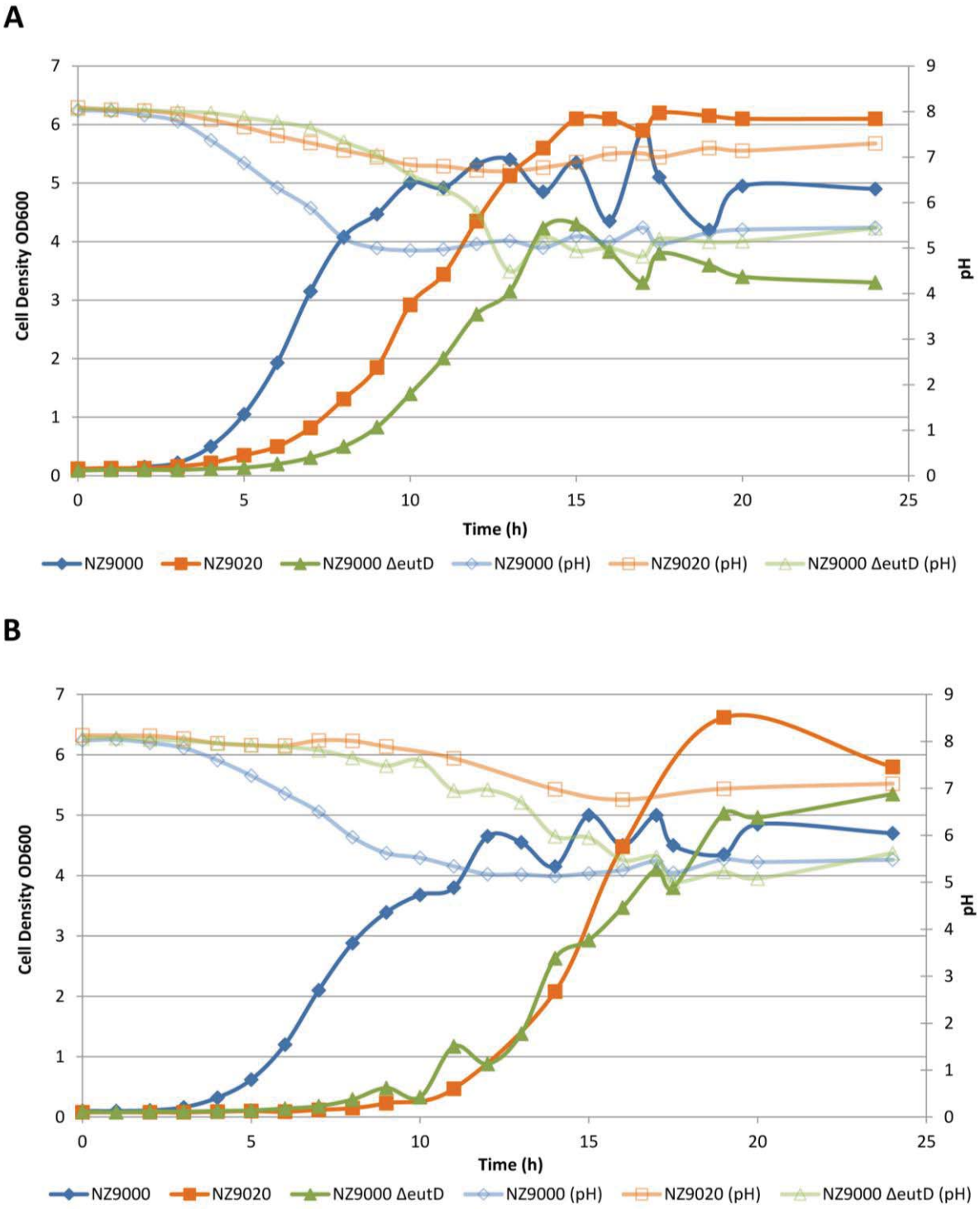

Figure 12. Growth curves of *L. lactis* NZ9000, NZ9020, & NZ9000 Δ*eutD* harbouring plasmids pNZ-CAB & pNZ-8148. *L. lactis* strains harbouring either (**A**) pNZ-8148 (vector control), or (**B**) pNZ-CAB (*phaCAB* operon) were grown under PHA accumulating conditions for 24 hours. The optical cell density of the cultures (measured at 600 nm) and pH of the growth medium was measured at specified time points. Experiments were performed in triplicate and the mean values are displayed (values are within 1 standard deviation).

3.3.2 Lactate and Acetate formation by recombinant *L. lactis*

The ability of the recombinant *L. lactis* strains (NZ9000, NZ9020, and NZ9000 Δ*eutD,* harbouring either the pNZ-CAB or pNZ-8148 plasmid) to produce acetate and lactate was assessed to investigate the *eutD* knockout phenotype and its effect on carbon flux. Strains were grown for 24 hrs under PHA accumulating conditions with samples of the culture supernatant taken at specified timepoints throughout the cultivation. The culture supernatant was then analysed for acetate and lactate content (2.13).

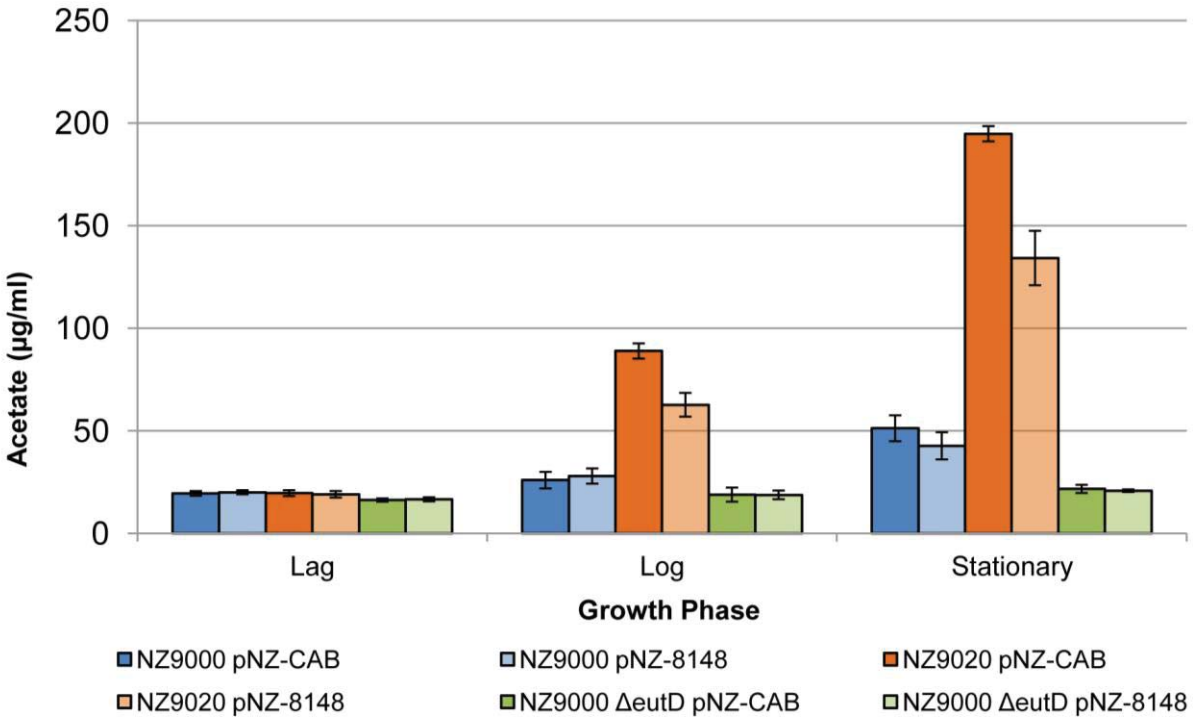

Figure 13. Acetate production by recombinant *L. lactis* NZ9000, NZ9020, & NZ9000 Δ*eutD* under PHA accumulating conditions. *L. lactis* strains harbouring either pNZ-8148 (vector control), or pNZ-CAB (*phaCAB* operon) were grown under PHA accumulating conditions for 24 hours. Samples were taken from the cell cultures at specified time points throughout the 24 hour period, cells were removed by centrifugation and the supernatant was assayed for acetate content. Experiments were performed in triplicate and the mean values are displayed.

It was expected that disruption of the phosphate acetyltransferase gene in *L. lactis* NZ9000 would lead to decreased production of acetate during cultivation when compared with the control strain (NZ9000). The results showed that irrespective of the plasmid expressed in the strain, the NZ9000 Δ*eutD* strain showed no significant

increase in acetate production over the 24 hour period in comparison to wildtype (NZ9000; Figure 13). As previously observed (Lee, 2011), the NZ9020 strain showed significant levels of acetate production relative to wildtype, which showed only a minor increase. For strains NZ9000 and NZ9000 Δ*eutD*, it was found that the presence of *pha*CAB within the expressed plasmid did not play a significant role in the level of acetate produced, indicating that the production of PHB does not significantly affect acetate production.

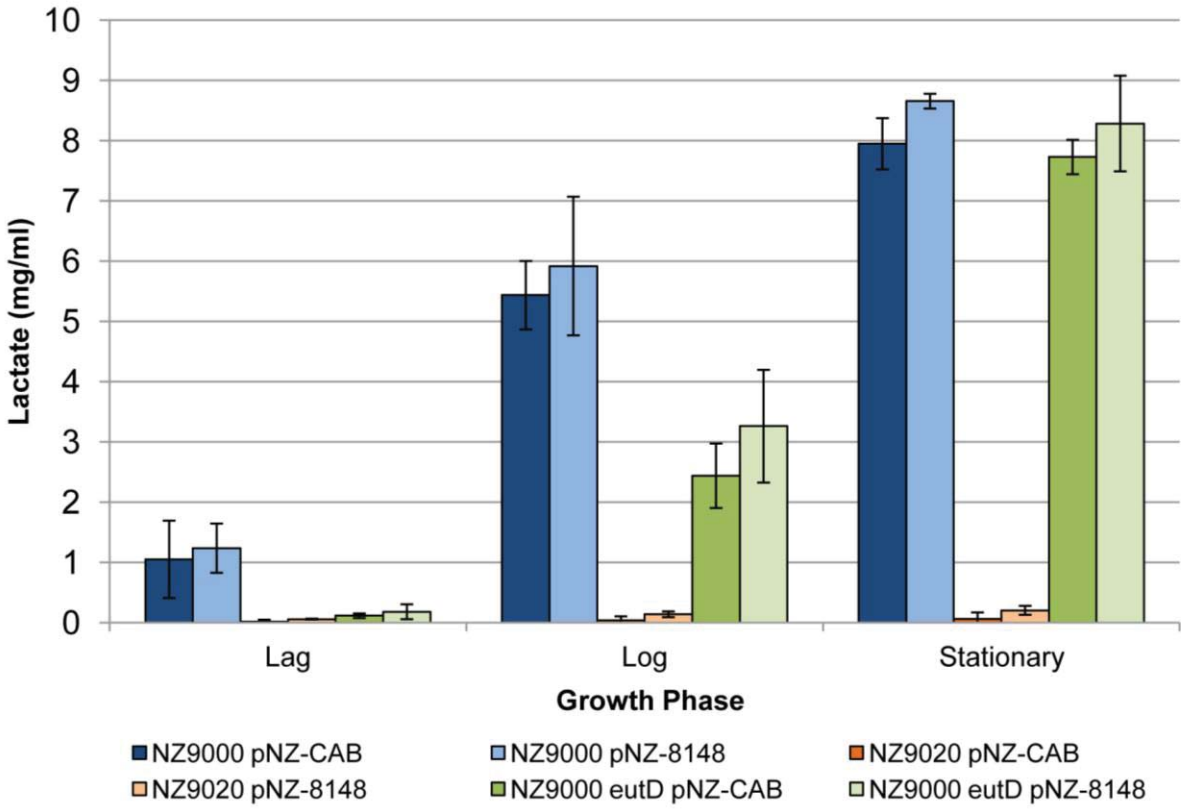

Figure 14. Lactate production by recombinant *L. lactis* NZ9000, NZ9020, & NZ9000 Δ*eutD* under PHA accumulating conditions. *L. lactis* strains harbouring either pNZ-8148 (vector control), or pNZ-CAB (*phaCAB* operon) were grown under PHA accumulating conditions for 24 hours. Samples were taken from the cell cultures at specified time points throughout the 24 hour period, cells were removed by centrifugation and the supernatant was assayed for lactate content. Experiments were performed in triplicate and the mean values are displayed.

After identifying decreased acetate levels as a phenotypic characteristic of the NZ9000 Δ*eutD* strain, the lactate levels were measured to assess if carbon from the pyruvate flux had been redistributed towards the lactate pathway (Figure 14). Lactate analysis indicated that the phosphate acetyltransferase deficient strain did not show a significant difference in the levels of lactate produced when compared with wildtype (NZ9000).

However as expected, the LDH deficient strain (NZ9020) showed significantly lower levels of lactate throughout the 24 hour period (Lee, 2011).

3.3.3 Quantification of PHB under PHA accumulating conditions

After observing the decreased acetate levels and unchanged lactate levels in the phosphate acetyltransferase knockout strain, it was hypothesized that the carbon normally distributed through the acetate pathway may have been redistributed towards increased production of acetyl-CoA. PHB production can be used as a way of indirectly measuring the intracellular availability of acetyl-Co-A.

To confirm whether PHB production was occurring and to quantify the PHB produced, GC/MS was used (2.12). *L. lactis* strains NZ9000 and NZ9000 Δ*eutD* harbouring either the pNZ-8148 or the pNZ-CAB plasmid were grown for 48 hours under PHA accumulating conditions and analysed by GC/MS. Results are displayed as a percentage of PHB per mg of cellular dry weight (CDW; Table 6). Results indicated that disruption of the phosphate acetyltransferase gene did not improve PHB accumulation. NZ9000 Δ*eutD* harbouring pNZ-CAB accumulated 10.11% of CDW compared with the positive control strain NZ9000 which accumulated 11.55% of CDW (Table 6). The negative controls showed no PHB production.

Table 6. GC/MS analysis of PHB accumulation in *L. lactis* NZ9000 and NZ9000 Δ*eutD*.

Samples	%PHB of CDW[a]
NZ9000 pNZ-CAB	**11.55**
NZ9000 pNZ-8148	**-**
NZ9000 eutD pNZ-CAB	**10.11**
NZ9000 eutD pNZ-8148	**-**

[a] Numbers based on single measurements.

In summary, the *eutD* gene was successfully knocked out in *L. lactis* NZ9000. Results showed that when deficient in phosphate acetyltransferase, PHB production has a positive effect on maximum cell density yet does not significantly affect media pH (Figure 12). Results also showed that the lack of phosphate acetetyltransferase had a negative impact on cell growth rate (Figure 12). Whilst lactate analysis of NZ9000 Δ*eutD* showed levels comparible to NZ9000 WT (Figure 14), acetate analysis revealed a significant reduction in acetate produced by NZ9000 Δ*eutD* compared with NZ9000 WT (Figure 13); this was expected as phosphate acetyltransferase is directly involved in the acetate pathway. GC/MS analysis showed that the NZ9000 Δ*eutD* strain harbouring pNZ-CAB produced less PHB than the positive control strain NZ9000 harbouring pNZ-CAB (Table 6).

3.4 Complementation of NZ9000 Δ*eutD* mutant

Once the *eutD* gene had been knocked out in the NZ9000 strain, the next step was to complement the mutant to restore the wildtype phenotype. To do this, primers were designed to amplify the full length *eutD* gene from NZ9000 (Table 4; 2.11.10). PCR products were separated using AGE with SYBR safe stain (2.11.6) and the fragment of the correct size (1147 bp) was gel-purified (2.11.7). This gene was then cloned into the pGEM-T Easy vector system (2.11.8) and transformed into *E. coli* XL1-Blue (2.10.1). Cells were plated onto LB agar plates containing 0.004% X-gal, 1 mM IPTG, 12.5 µg/mL tetracycline and 75 µg/mL ampicillin (2.4.1). Single white colonies were selected for plasmid isolation (2.11.1) and RE analysis using *Nco*I and *Sac*I (2.11.5). After complete digestion, the fragments were visualised using AGE (2.11.6), and plasmids displaying the correct band pattern (3028 bp and 1147 bp; results not shown) were sent for sequence analysis (2.11.11).

After sequence confirmation, the *eutD* gene was excised from pGEM-T Easy by RE digest using *Nco*I and *Sac*I (2.11.5). This fragment was ligated into the similarly digested pNZ-8148 plasmid (2.11.9). The ligation product was used to transform *E. coli* XL1-Blue (2.10.1), and cells were plated onto LB agar containing 12.5 µg/mL tetracycline and 10 µg/mL chloramphenicol (2.4.1). Single colonies were selected for plasmid isolation (2.11.1) and RE analysis using *Sac*I (2.4.1). However, after complete digestion and visualisation using AGE no plasmids displayed the correct band pattern; thus complementation of the *eutD* knockout strain was not able to be assessed.

Part II: NZ9000 Δ*adhE*

3.5 Construction of an *adhE* knockout plasmid

To construct an *adhE*::*tet* replacement strain of *L. lactis* NZ9000, a plasmid was constructed that allowed for the selection of the desired mutant through the occurence of a double cross-over event on both flanking regions of the *adhE* gene. Plasmid pUC_*adhE*5'_Tet^R_*adhE*3' was constructed containing, a 5' fragment and a 3' fragment of the *adhE* gene flanking an internal tetracycline resistance cassette. Contruction of this plasmid was a multi step process (Figures 5 & 6).

First, primers were designed to amplify a 510 bp fragment containing a 5' section of the *adhE* gene as well as a 491 bp fragment containing a 3' section of the *adhE* gene (Table 4). These primers were used in PCR reactions with linearized NZ9000 *L. lactis* genomic DNA as a template (2.11.10). In addition, primers were designed to amplify a tetracycline resistance gene from the pT181 plasmid (Maguin et al., 1996) (Table 4). These primers were used in a PCR reaction with whole plasmid as a template. Fragments of the correct size (510 bp for adhE5'; 491 bp for adhE3'; 1800 bp for Tet^R; results not shown) generated from the three PCR reactions were separated using AGE with SYBR safe stain (2.11.6) and gel purified (2.11.7).

The second step involved cloning the fragments into the pGEM-T Easy vector system to allow for the fragments to be sequenced. After ligation into pGEM-T Easy (2.11.8), the products were transformed into *E. coli* XL1-Blue (2.10.1) and plated onto LB agar plates containing 4% X-gal, 1 mM IPTG, 12.5 µg/mL tetracycline and 75 µg/mL ampicillin (2.4.1). Single white colonies were isolated and cultured for plasmid isolation (2.11.1) and RE analysis (*Eco*RI for *adhE* fragments; *Bam*HI for TetR; 2.11.5). After complete digestion, AGE was used to visualise the fragments: two fragments of expected size 510 bp and 2997 bp were seen for *adhE*5', two fragments of expected size 491 bp and 2997 bp were seen for *adhE*3', and two fragments of expected size 1800 bp and 3030 bp were seen for Tet^R; results not shown. Plasmids displaying the correct band pattern were sent for sequence analysis (2.11.11).

Once all fragments had been confirmed by sequencing, they were ligated together into one pGEM-T Easy vector. First the pGEM-T Easy vector was linearised by RE digest

using *Eco*RI, isolated and purified from agarose gel, and treated with Antarctic phosphatase to prevent religation of the vector (2.11.9.1). The *adhE*5' and *adhE*3' fragments were excised from the pGEM-T Easy adhE5' and adhE3' vectors by RE digest using *Eco*RI and *Bam*HI, isolated and gel purified (2.11.6-7). The *adhE*5' and *adhE*3' fragments were then ligated into the *Eco*RI site of the pGEM-T Easy vector using T4 DNA ligase (2.11.9). The ligation product was transformed into *E. coli* XL1-Blue (2.10.1) and plated onto LB agar containing 4% X-gal, 1 mM IPTG, 12.5 µg/mL tetracycline and 75 µg/mL ampicillin (2.4.1). Single white colonies were isolated and cultured for plasmid isolation (2.11.1) and RE analysis using *Eco*RI; two fragments of expected size 1013 bp and 2997 bp were seen after complete digestion using AGE (2.11.6; results not shown). Plasmid displaying the correct restriction pattern was isolated and linearised by RE digest using *Bam*HI, purified from agarose gel and treated with Antarctic phosphatase to prevent religation of the vector (2.11.9.1). The Tet^R gene was excised from the pGEM-T Easy_TetR vector by RE digest using *Bam*HI, isolated and purified from agarose gel using gel purification (2.11.7). The Tet^R gene was then ligated into the *Bam*HI site of the pGEM-T Easy_*adhE*5'_*adhE*3' vector using T4 DNA ligase (2.11.9). The ligation product was transformed into *E. coli* XL1-Blue (2.10.1) and plated onto LB agar containing 4% X-gal, 1 mM IPTG, 12.5 µg/mL tetracycline and 75 µg/mL ampicillin (2.4.1). Single white colonies were selected for plasmid isolation (2.11.1) and RE analysis using *Eco*RI; two fragments of expected size 820 bp and 2997 bp were seen after complete digestion using AGE (2.11.6; results not shown).

The final step in constructing pUC_ *adhE*5'_Tet^R_ *adhE*3' involved excising the *adhE*5'_Tet^R_ *adhE*3' fragment from pGEM-T Easy_adhE5'-TetR-adhE3' by RE digest using *Eco*RI (2.11.5). The fragment was separated using AGE with SYBR safe stain (2.11.6) and gel purified (2.11.7). The fragment was then ligated into the *Eco*RI site of the linearised pUC19_cm^R vector (2.11.9). The ligation product was transformed into *E. coli* XL1-Blue (2.10.1) and plated onto LB agar containing 12.5 µg/mL tetracycline and 5 µg/mL chloramphenicol (2.4.1). Single colonies were selected for plasmid isolation (2.11.1) and RE analysis using *Bgl*I (2.11.5); two fragments of expected size 2044 bp and 4388 bp were seen after complete digestion using AGE (2.11.6; Figure 15).

3.6 Construction of the NZ9000 Δ*adhE* mutant

The first step in constructing the NZ9000 Δ*adhE* knockout strain was electroporation of pUC_ *adhE*5'_Tet^{R}_ *adhE*3' into NZ9000 (Figure 7; 2.10.2). After electroporation, the *L. lactis* cells were plated onto solid GM17 agar containing 5 µg/mL tetracycline (2.4). Single colonies were selected and plated both onto fresh GM17 agar containing either 5 µg/mL tetracycline or 5 µg/mL tetracycline and 10 µg/mL chloramphenicol. Colonies that grew on the tetracycline plates but did not grow on the tetracycline and chloramphenicol plates were selected and cultured in liquid GM17 media containing 5 µg/mL tetracycline. Colonies that displayed tetracycline resistance and chloramphenicol sensitivity likely resulted from a one-step double cross-over event on both flanking regions of the *adhE* gene, and thus should have contained the *adhE*::*tet* replacement mutation. After overnight cultivation, genomic DNA was isolated from the cells (2.11.2) and linearized by digestion with *Bsm*AI (2.11.5). The linearized DNA was then subjected to PCR (2.11.10) using primers targeting regions outside of the *adhE* recombination sites (Table 4). WT NZ9000 DNA was also linearized by digestion with *Bsm*AI and subjected to the same PCR cycle as a control. All fragments generated from the PCR reactions were separated using AGE and SYBR safe stain (2.11.6). However, no fragments of the expected size (4136 bp) for the incorporation of the tetracycline resistance cassette were observed. Only fragments consistent with the uninterrupted WT *adhE* gene were seen (3373 bp; Figure 16), indicating that this construct was unable to successfully replace the *adhE* gene.

In a second attempt, primers were designed for the amplification of new *adhE* flanking regions (Table 4) and used to make a new knockout plasmid following the same steps as outlined above. However, this plasmid was also unsuccessful at knocking out the *adhE* gene

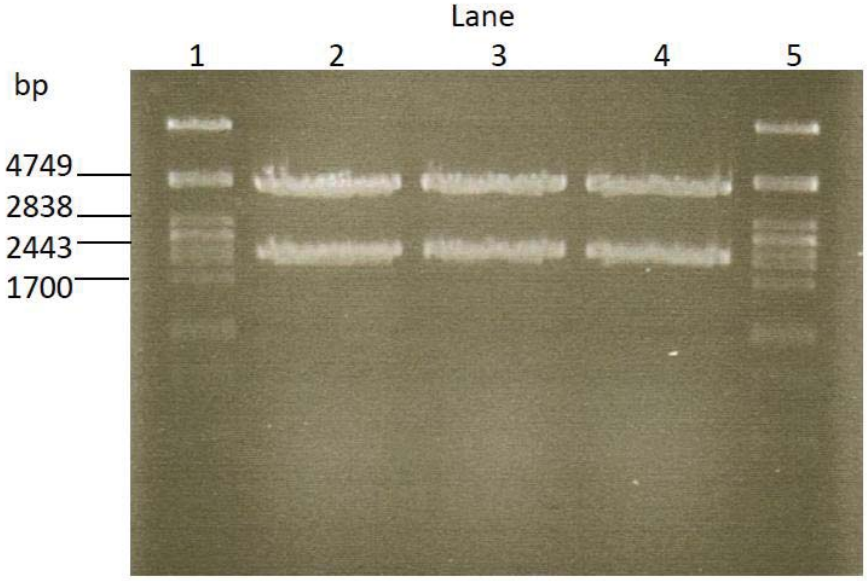

Figure 15. Restriction analysis of plasmid isolated from *E. coli* XL1-Blue cells transformed with pUC_*adhE*5'_Tet^R_*adhE*3'. Lanes 1 & 5, DNA ladder standard (λ *Pst*I); Lanes 2 – 4, isolated plasmid digested with *Bgl*I with expected sizes of 2044 bp and 4388 bp (complete digestion). Plasmid containing no insert runs at the expected size of 1456 bp and 2044 bp.

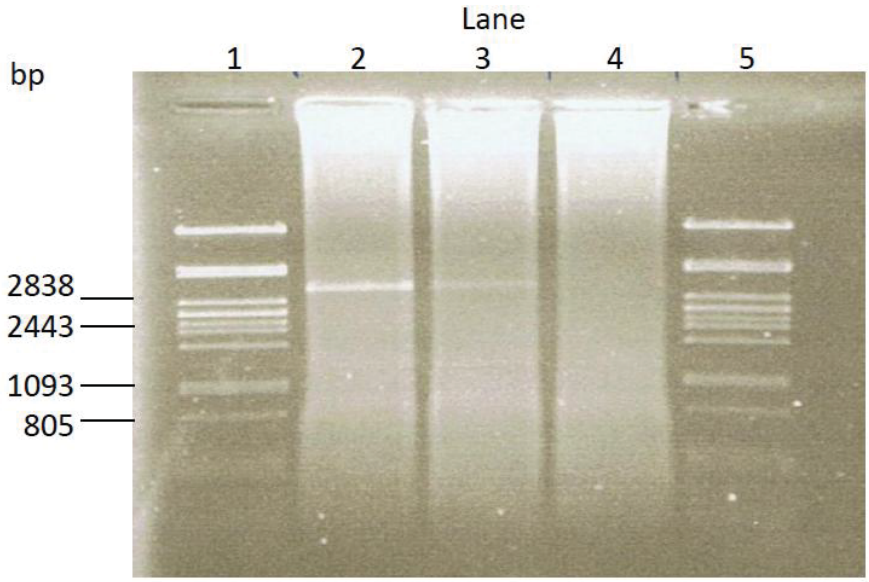

Figure16. PCR analysis of NZ9000 and NZ9000 Δ*adhE* genomic DNA. Lanes 1 & 5, DNA ladder standard (λ *Pst*I); Lane 2, NZ9000 PCR with expected size 3373 bp; Lanes 3 & 4, NZ9000 Δ*adhE* PCR with expected size 3526 bp.

CHAPTER 4: DISCUSSION

The production of PHB granules in a Gram-positive host eliminates the need for LPS endotoxin removal, making the beads suitable for biomedical applications. *L. lactis* is particularly suitable due to it being a food grade GRAS organism with a variety of genetic tools readily available. However, production of PHB in *L. lactis* has relatively poor yields (6% (wt/wt) of CDW) when compared with yields from recombinant *E. coli* (60-80% (wt/wt) of CDW) (Mifune et al., 2009). Mifune and coworkers suggested that to improve the PHB yield for *L. lactis* it would be advisable to monitor metabolic fluxes and possibly look at modifying the expression strengths of the individual *pha* genes. Gene dosage was shown to greatly increase the PHB accumulation of *C. glutamicum* (Jo et al., 2007), and so logically it would be valuable to assess the potential effects of gene dosage in *L. lactis*.

In this project we investigated the hypothesis that PHB yield could be improved by modifying the pathways involved in the metabolic flux from pyruvate. This hypothesis has previously been partially assessed using two *L.* lactis mutant strains NZ9010 and NZ9020 (Lee, 2011). NZ9010 and NZ9020 are both derivatives of NZ9000 with a single *ldh* gene knockout and double *ldh* knockout (*ldh* and *ldhB*), respectively. Results from this study showed that neither of the *ldh* deficient strains increased PHB production; instead they had a negative impact, dropping PHB accumulation to 0-0.04% (wt/wt) compared with NZ9000 (3.57% wt/wt) (Lee, 2011).

To further investigate this hypothesis, two candidate genes (*adhE* and *eutD* encoding acetaldehyde dehydrogenase and phosphate acetyltransferase respectively) were selected that if knocked out, might improve the accumulation of acetyl CoA, thus increasing the PHB precursor pool and consequently improving PHB production. However after several attempts at electroporation, optimisation of the procedure and targeting of different flanking regions, one of these genes, *adhE*, was not able to be knocked out. This was unexpected as it had previously been shown that *L. lactis* NZ9000 could survive without a fully functional acetaldehyde dehydrogenase (Arnau et al., 1998). This suggests a problem with the chosen target regions and/or knockout method for this particular gene, as opposed to the non-viability of an acetaldehyde dehydrogenase-deficient strain.

However, the *eutD* gene was successfully knocked out after electroporation into NZ9000. A number of parameters were measured to characterise the *eutD* deficient strain, including growth rate, cell density at stationary growth phase, pH, PHB accumulation, and production of acetate and lactate. These parameters were assessed over a 24 hr period under conditions of PHA accumulation. The NZ9000 Δ*eutD* strain was the only strain in which presence of the PHB production plasmid affected the growth characteristics. Results showed that when harbouring the pNZ-CAB plasmid (PHB production), the culture reached a maximum cell density of approximately 5 yet only reached approximately 3.2 when harbouring the pNZ-8148 plasmid; pH was unaffected (Figure 12). This suggests that when deficient in phosphate acetyltransferase, PHB production has a positive effect on maximum cell density. Results also showed that PHB production does not significantly affect media pH, as no significant differences were seen in strains harbouring either plasmid (Figure 12). It was also noted that the growth rate of NZ9000 Δ*eutD* was considerably slower than that observed for NZ9000 when harbouring pNZ-8148, indicating that a deficiency in phosphate acetyltransferase has a negative impact on cell growth rate (Figure 12). As previously shown (Lee, 2011), the NZ9020 strain reached higher cell densities than the WT strain which is likely attributable to the high pH of the media, as a lower media pH as seen for NZ9000 may have an inhibitory effect on growth (Figure 12;(Mifune et al., 2009). Change in the pH of the media is primarily caused by the synthesis of lactic acid as a fermentation product (Hoefnagel et al., 2002a). Culture pH levels suggest that NZ9020 produces less lactate than NZ9000 and NZ9000 Δ*eutD*, both of which appear to have similar lactate levels. This initial phenotype was confirmed by lactate analysis of the culture medium for all strains, with the levels of lactate produced correlating to the changes in media pH. NZ9020 produced insignificant levels of lactate (<0.5 mg/mL) in comparison to NZ9000 and NZ9000 Δ*eutD* (7.5-9.1 mg/mL; Figure 14).

After confirming the previously noted NZ9020 phenotype (Lee, 2011) and establishing a phenotype for NZ9000 Δ*eutD*, it was necessary to measure other metabolites in the growth medium to determine if redistribution of the carbon flux from pyruvate towards products such as acetate or acetyl-CoA had occurred. Acetate analysis of the culture medium showed significantly higher levels of acetate for NZ9020 than for the control (NZ9000; Figure 13) as expected (Hoefnagel et al., 2002a; Lee, 2011). However, there

was an unexpected increase in levels of acetate in NZ9020 when harbouring pNZ-CAB (PHB production) than when harbouring pNZ-8148 (negative control); PHB production was expected to have a negative impact on acetate accumulation due to the redirection of available acetyl CoA towards PHB biogenesis (Figure 3; (Lee, 2011)). It is important to note the considerable reduction in acetate produced by NZ9000 Δ*eutD* (<25 μg/mL) compared with NZ9000 WT (42-52 μg/mL; Figure 13). This was expected as the phosphate acetyltransferase is directly involved in the acetate pathway (Figure 3), and suggests that the carbon flux has been redistributed elsewhere in the pyruvate pathway.

It was expected that the decrease in acetate production and unchanged lactate levels would lead to increased production of PHB in NZ9000 Δ*eutD* due to the redistribution of carbon towards increased acetyl CoA accumulation. Therefore, GC/MS analysis was used to quantify the PHB produced. Results showed that the positive control strain NZ9000 harbouring pNZ-CAB produced 11.55 % PHB per mg of dry weight (Table 6), which is higher than the 6 % (wt/wt) previously published by Mifune *et al.* (2009) and considerably higher than the 3.57% (wt/wt) reported by Lee (2011). All negative controls were showed no PHB accumulation. Interestingly, the NZ9000 Δ*eutD* strain harbouring pNZ-CAB produced less PHB, with a yield of 10.11 % per mg of dry weight. This was unexpected; it suggests that the carbon redistribution was not towards acetyl CoA accumulation, but towards other products in the pathway.

It could therefore prove valuable to measure the levels of other metabolites produced, such as acetoin and ethanol, to determine where the carbon has been redistributed. However, it is also possible that acetyl CoA levels did increase, but PHB yied did not subsequently increase; this could potentially be due to a rate limiting step in the PHB biogenesis pathway. Metabolic pathways have a fixed capacity; branches with a low capacity may be unable to utilise all of the increased carbon flow. It has previously been shown that gene dosage of the *pha*CAB genes can have a significant effect on PHB production in recombinant bacterial strains (Jo et al., 2007). Therefore it may be advisable to modify the expression of these genes in recombinant *L. lactis* through gene dosage, for example by increasing plasmid copy numbers.

To fully characterise the NZ9000 Δ*eutD* strain and confidently assign functionality to the *eutD* gene, it is necessary to complement the mutant to ensure that WT function is

restored and to confirm that only the targeted gene was affected. This was attempted through the construction of a pNZ-8148 plasmid containing the full length NZ9000 *eutD* gene (primers eutD NF and eutD SR; Table 4). However, difficulties were encountered when constructing this plasmid and consequently complementation was not assessed. Sequencing data for the *eutD* PCR product showed the fragment had the correct sequence; however, the successful ligation of this fragment into the pNZ-8148 plasmid was not achieved. It would be valuable to reassess the cutting efficiency of the enzymes used and/or design new primers that use different RE sites. Due to complementation not being asessed, we cannot confirm that the phenotype observed for NZ9000 Δ*eutD* was due to disruption of the target *eutD* gene or whether it is the result of accidental disruption of another mechanism. Therefore it is essential that the NZ9000 Δ*eutD* strain is complemented to validate the preliminary conclusions drawn from this experiment.

CHAPTER 5: CONCLUSIONS AND FUTURE WORK

Contrary to the hypothesis, PHB production using a strain deficient in phosphate acetyltransferase did not result in increased PHB production compared with NZ9000. The NZ9000 Δ*eutD* strain showed PHB levels similar to those of NZ9000 despite having significantly lower levels of acetate. This suggests that carbon from the acetate pathway is not being redistributed towards increased acetyl CoA levels as desired, but rather is diverted elsewhere in the pathway. Metabolic processes are very complex, and it is often difficult to identify the specific enzymes that need to be altered to generate the desired effects. Assessing the levels of other metabolites in the pathway to determine where the excess carbon has been directed could potentially identify new target genes for influencing acetyl CoA levels. It would also be valuable to investigate the effects of modifying gene expression levels of the *pha* genes, for example through gene dosage using increased plasmid copy numbers.

PHB production using a strain deficient in acetaldehyde dehydrogenase (*adhE*) was not assessed due to difficulties encountered in creating the knockout strain. An *adhE* deficient strain has the potential to increase PHB production. However, our failure to produce the strain suggests that different knockout strategies need to be investigated, for example targeting different regions of the gene for recombination or placing the *adhE* gene under the control of an inducible promoter.

Another potential means of increasing PHB accumulation could include using the *eutD* knockout plasmid to knockout out the *eutD* gene in NZ9020, creating an Δ*eutD*Δ*ldh* strain. This strain has the potential to greatly increase the levels of available acetyl CoA; however the lack of acetate and lactate pathways could be detrimental to the viability of the strain.

Overall, this study showed the successful construction and phenotypic characterisation of a phosphate acetyltransferase deficient strain of *L. lactis*. Production of acetate was substantially reduced in this mutant, and PHB production was successfully established. However, rather than increasing, levels of PHB production by the eutD knockout were comparable to WT. Additionally, complementation of the mutant strain still needs to be achieved to confirm that the observed acetate-production phenotype is attributable to

the lack of the *eutD* gene. As an *eutD* mutant alone did not increase PHB yield in *L. lactis*, other approaches will be necessary to achieve this goal. Potential future developments include double knockout strains and altered *pha* gene dosage.

REFERENCES

Arnau, J., Jørgensen, F., Madsen, S.M., Vrang, A., and Israelsen, H. (1998). Cloning of the Lactococcus lactis adhE gene, encoding a multifunctional alcohol dehydrogenase, by complementation of a fermentative mutant of Escherichia coli. Journal of Bacteriology *180*, 3049-3055.

Backstrom, B.T., Brockelbank, J.A., and Rehm, B.H.A. (2007). Recombinant Escherichia coli produces tailor-made biopolyester granules for applications in fluorescence activated cell sorting: functional display of the mouse interleukin-2 and myelin oligodendrocyte glycoprotein. Bmc Biotechnology *7*.

Banki, M.R., Gerngross, T.U., and Wood, D.W. (2005). Novel and economical purification of recombinant proteins: Intein-mediated protein purification using in vivo polyhydroxybutyrate (PHB) matrix association. Protein Science *14*, 1387-1395.

Barnard, G.C., McCool, J.D., Wood, D.W., and Gerngross, T.U. (2005). Integrated recombinant protein expression and purification platform based on Ralstonia eutropha. Applied and Environmental Microbiology *71*, 5735-5742.

Bongers, R.S., Hoefnagel, M.H.N., Starrenburg, M.J.C., Siemerink, M.A.J., Arends, J.G.A., Hugenholtz, J., and Meerebezem, M. (2003). IS981-mediated adaptive evolution recovers lactate production by ldhB transcription activation in a lactate dehydrogenase-deficient strain of Lactococcus lactis. Journal of Bacteriology *185*, 4499-4507.

Chen, G.Q., and Wu, Q. (2005). The application of polyhydroxyalkanoates as tissue engineering materials. Biomaterials *26*, 6565-6578.

Cocaign-Bousquet, M., Even, S., Lindley, N.D., and Loubiere, P. (2002). Anaerobic sugar catabolism in *Lactococcus lactis*: genetic regulation and enzyme control over pathway flux. Applied Microbiology and Biotechnology *60*, 24-32.

De Vos, W.M., and Hugenholtz, J. (2004). Engineering metabolic highways in Lactococci and other lactic acid bacteria. Trends in Biotechnology *22*, 72-79.

Grage, K., Jahns, A.C., Parlane, N., Palanisamy, R., Rasiah, I.A., Atwood, J.A., and Rehm, B.H.A. (2009). Bacterial polyhydroxyalkanoate granules: Biogenesis, structure, and potential use as nano-/micro-beads in biotechnological and biomedical applications. Biomacromolecules *10*, 660-669.

Hazer, B., and Steinbuchel, A. (2007). Increased diversification of polyhydroxyalkanoates by modification reactions for industrial and medical applications. Applied Microbiology and Biotechnology *74*, 1-12.

Hoefnagel, M.H.N., Starrenburg, M.J.C., Martens, D.E., Hugenholtz, J., Kleerebezem, M., Van Swam, II, Bongers, R., Westerhoff, H.V., and Snoep, J.L. (2002a). Metabolic engineering of lactic acid bacteria, the combined approach: kinetic modelling, metabolic control and experimental analysis. Microbiology-Sgm *148*, 1003-1013.

Hoefnagel, M.H.N., van der Burgt, A., Martens, D.E., Hugenholtz, J., and Snoep, J.L. (2002b). Time dependent responses of glycolytic intermediates in a detailed glycolytic model of *Lactococcus lactis* during glucose run-out experiments. Molecular Biology Reports *29*, 157-161.

Jiang, W., Papa, E., Fischer, H., Mardyani, S., and Chan, W.C.W. (2004). Semiconductor quantum dots as contrast agents for whole animal imaging. Trends in Biotechnology *22*, 607-609.

Jo, S.J., Maeda, M., Ooi, T., and Taguchi, S. (2006). Production system for biodegradable polyester polyhydroxybutyrate by Corynebacterium glutamicum. Journal of Bioscience and Bioengineering *102*, 233-236.

Jo, S.J., Matsumoto, K., Leong, C.R., Ooi, T., and Taguchi, S. (2007). Improvement of Poly(3-Hydroxybutyrate) [P(3HB)] Production in *Corynebacterium glutamicum* by Codon Optimization, Point Mutation and Gene Dosage of P(3HB) Biosynthetic Genes. Journal of Bioscience and Bioengineering *104*, 457-463.

Karhanek, M., Kemp, J.T., Pourmand, N., Davis, R.W., and Webb, C.D. (2005). Single DNA molecule detection using nanopipettes and nanoparticles. Nano Letters *5*, 403-407.

Lee, J. (2011). Molecular characterisation of PHA synthase and the *in vivo* synthesis of functionalised PHA beads with surface immobilised PHA beads with surface immobilised proteins. In IMBS (Palmerston North, Massey University).

Lee, S.Y., Lee, K.M., Chang, H.N., and Steinbuchel, A. (1994). Comparison of recombinant *Escherichia coli* strains for synthesis and accumulation of poly-(3-hydroxybutyric acid) and morphological changes. Biotechnology and Bioengineering *44*, 1337-1347.

Madison, L.L., and Huisman, G.W. (1999). Metabolic engineering of poly(3-hydroxyalkanoates): From DNA to plastic. Microbiology and Molecular Biology Reviews *63*, 21-53.

Maguin, E., Prevost, H., Ehrlich, S.D., and Gruss, A. (1996). Efficient insertional mutagenesis in lactococci and other gram-positive bacteria. Journal of Bacteriology *178*, 931-935.

Mierau, I., and Kleerebezem, M. (2005). 10 years of the nisin-controlled gene expression system (NICE) in Lactococcus lactis. Applied Microbiology and Biotechnology *68*, 705-717.

Mifune, J., Grage, K., and Rehm, B.H.A. (2009). Production of Functionalized Biopolyester Granules by Recombinant Lactococcus lactis. Applied and Environmental Microbiology *75*, 4668-4675.

Panyam, J., and Labhasetwar, V. (2003). Biodegradable nanoparticles for drug and gene delivery to cells and tissue. Advanced Drug Delivery Reviews *55*, 329-347.

Papin, J.A., Price, N.D., Wiback, S.J., Fell, D.A., and Palsson, B.O. (2003). Metabolic engineering the the post-genome era. Trends in Biochemical Sciences *28*, 250-258.

Parlane, N.A., Grage, K., Lee, J.W., Buddle, B.M., Denis, M., and Rehm, B.H.A. (2011). Production of a Particulate Hepatitis C Vaccine Candidate by an Engineered Lactococcus lactis Strain. Applied and Environmental Microbiology *77*, 8516-8522.

Parlane, N.A., Grage, K., Mifune, J., Basaraba, R.J., Wedlock, D.N., Rehm, B.H.A., and Buddle, B.M. (2012). Vaccines Displaying Mycobacterial Proteins on Biopolyester Beads Stimulate Cellular Immunity and Induce Protection against Tuberculosis. Clin Vaccine Immunol *19*, 37-44.

Platteeuw, C., Hugenholtz, J., Starrenburg, M., Vanalenboerrigter, I., and Devos, W.M. (1995). Metabolic engineering of *Lactococcus lactis* - influence of the overproduction of alpha-acetolactate synthase in strains deficient in lactate-dehydrogenase as a function of culture conditions. Applied and Environmental Microbiology *61*, 3967-3971.

Rehm, B.H.A. (2003). Polyester synthases: natural catalysts for plastics. Biochemical Journal *376*, 15-33.

Rehm, B.H.A. (2006). Genetics and biochemistry of polyhydroxyalkanoate granule self-assembly: The key role of polyester synthases. Biotechnology Letters *28*, 207-213.

Sanford, K., Soucaille, P., Whited, G., and Chotani, G. (2002). Genomics to fluxomics and physiomics-pathway engineering. Current Opinion in Microbiology *5*, 318-322.

Soukka, T., Härmä, H., Paukkunen, J., and Lövgren, T. (2001). Utilization of kinetically enhanced monovalent binding affinity by immunoassays based on multivalent nanoparticle-antibody bioconjugates. Analytical Chemistry *73*, 2254-2260.

Starrenburg, M.J.C., and Hugenholtz, J. (1991). Citrate fermentation by *Lactococcus* and *Leuconostoc* spp. Applied and Environmental Microbiology *57*, 3535-3540.

Swindell, S.R., Benson, K.H., Griffin, H.G., Renault, P., Ehrlich, S.D., and Gasson, M.J. (1996). Genetic manipulation of the pathway for diacetyl metabolism in *Lactococcus lactis*. Applied and Environmental Microbiology *62*, 2641-2643.

Valappil, S.P., Boccaccini, A.R., Bucke, C., and Roy, I. (2007). Polyhydroxyalkanoates in Gram-positive bacteria: Insights from the genera Bacillus and Streptomyces. Antonie van Leeuwenhoek, International Journal of General and Molecular Microbiology *91*, 1-17.

Zou, X.H., and Chen, G.Q. (2007). Metabolic engineering for microbial production and applications of copolyesters consisting of 3-hydroxybutyrate and medium-chain-length 3-hydroxyalkanoates. Macromolecular Bioscience *7*, 174-182.